Subsidence in rift zones

Analyzing results from repeated precision leveling of the Vogar Profile on the Reykjanes Peninsula, Southwest Iceland

Ingrid Anell

Examensarbeten i Geologi vid
Lunds universitet - Berggrundsgeologi, nr. 178

Geologiska institutionen
Centrum för GeoBiosfärsvetenskap
Lunds universitet
2004

L, L.

Subsidence in rift zones

Analyzing results from repeated precision leveling of the Vogar Profile on the Reykjanes Peninsula, Southwest Iceland

Ingrid Anell

Anell, I., 2004: Subsidence in rift zones; Analyzing results from repeated precision leveling of the Vogar Profile on the Reykjanes Peninsula, Southwest Iceland. M.Sc. Thesis in Geology at the University of Lund. Nr. 178

Abstract

The mid-Atlantic ridge connects with land at the Reykjanes peninsula, Southwest Iceland. Iceland extends well over the whole ridge and allows for representative surface observations of sea-floor processes. Across the Peninsula the plate boundary is characterized by a rift zone, which encompasses leaky transform fault zone characteristics. Across a fissure swarm, connected with the Reykjanes volcanic system, the Vogar leveling profile extends. Precision leveling was conducted along the line in 1966, 1968, 1969, 1971 and 1976. The profile was re-measured in 2004 and it was aimed to observe various aspects of subsidence in the rift zone.

Subsidence along the profile is the result of the effect of two main components. The first being influence from the central axis of the plate boundary causing the southeastern end of the profile to subside at a higher rate then the northwestern end, averaging 1.1mm/yr. The second being the influence from the local fissure swarm causing the central part of the profile to subside due to movement on two boundary faults.

Annual rates of subsidence are not constant but are related to the size of appreciable fault movements. In 1966-1968 and 1971-1976, annual subsidence rates were higher and in 1976-2004 lower than average.

Prominent fault movements are earthquake related. 1976-2004 was a calm period following the stress release by several earthquake swarms between 1971 and 1976. One prominent, unconfirmed, fault movement occurred between 1976 and 2004, presumably triggered by the two large earthquakes in the South Iceland Seismic Zone in 2000.

At several faults local progressive faulting is occurring with subsidence of a single benchmark on the down-throw side of a fault. This occurs at most faults and is the result of movement of semi-detached fault blocks within the 'disturbed' zone sliding down along the fault plane.

Modeling the subsidence results for the Vogar profile in relation to the central plate axis proved too complex for the simple linear pressure decrease model when comparing with the GPS data obtained for a benchmark along the profile. This GPS data indicated a minimum subsidence of this benchmark of 3mm/yr. The best fit for points affected only by the regional component gave an annual subsidence at the rift of 5.5mm/yr and a locking depth of 3.8km, which did not correlate with GPS data. Presumably the effect of the local component overprints the regional component or the GPS data for the last 11 years is not representative of the last 38 years.

Keywords: Iceland, Reykjanes Peninsula, Vogar profile, precision leveling, faulting, subsidence, modeling subsidence, Mogi model.

Ingrid Anell, Department of Geology, Geobiosphere Science Centre, the University of Lund, Sölvegatan 12, 223 62 Lund.

Subsidens i riftzoner

Analys av resultat från precisionshöjdmätningar längs Vogarprofilen på Reykjanes halvön, sydvästra Island

Ingrid Anell

Sammanfattning

På Reykjanes halvön i sydvästra Island får den mittatlantiska ryggen förbindelse med land. Eftersom Island sträcker sig över hela ryggen kan man studera oceanbottenspridning på fast mark. På halvön utgörs plattgränsen av en riftzon kombinerad med en transform rörelse. Vogarprofilen utgörs av en precisionsavvägd profil som dragits över en sprickzon i rät vinkel mot plattgränsens centralaxel. Precisionshöjdmätningar längs denna profil gjordes 1966, 1968, 1969, 1971 och 1976. Mätningen upprepades 2004 för att studera hur jordskorpan sjunker i riftzonen.

De årliga nedsänkningshastigheterna är inte konstanta utan beror på storleken på förkastningsrörelserna. 1966-1968 och 1971-1976 var den årliga hastigheten högre medan 1976-2004 var den lägre än normalt.

Större förkastningsrörelser sker på grund av jordbävningar. 1976-2004 var en lugn period som följde på en period av strainutlösning kännetecknad av flera jordbävningssvärmar mellan 1971 och 1976. En stor, men obekräftad förkastningsrörelse skedde mellan 1976 och 2004, förmodligen utlöst av två stora jordbävningar i den sydisländska seismikzonen år 2000.

Vid flera av förkastningarna sker fortlöpande lokala förkastningsrörelser. Därvid sjunker en enskild mätpunkt på den nedförkastade sidan av förkastningslinjen. Detta sker vid de flesta förkastningarna och är ett resultat av att ett till hälften lösgjort block glider ner längs förkastningen i en störningszon.

Två komponenter påverkar hur jordskorpan sjunker. Den första är regional och orsakad av plattgränsens centralaxel medan den andra är lokal orsakad av sprickzonen. Den regionala komponenten medför att profilens sydöstra del sjunker med en hastighet som är 1,1 mm/år högre än dess nordvästra. Den lokala komponenten gör att sprickzonens centrala del sjunker på grund av förkastningsrörelser på två av de avgränsande förkastningarna.

Det går inte att modellera nedsänkningen längs Vogarprofilen med enkel modell baserad på en linjär tryckminskning från den centrala plattgränsen. Detta är tydligt då man tar hänsyn till GPS data som erhållits för en av mätpunkterna längs profilen. GPS data ger en miniminedsänkning för denna punkt på 3 mm/år. Den bästa anpassningen för datapunkterna får man för en nedsänkning vid plattgränsen uppgående till 5,5 mm/år och ett blockeringsdjup uppgående till 3,8 km. Dessa data överensstämmer inte med erhållna GPS data. Förmodligen finns det en lokal nedsänkningskomponent som omfattar Reykjanessprickzonen och medför att denna sänks ytterligare 2 mm/år. GPS har använts för att bestämma den absoluta nedsänkningen. GPS-data finns endast från en elvaårsperiod medan avvägningsdata omfattar en period om 38 år. Det är klarlagt att rörelserna inte sker med jämn hastighet. Detta innebär att data från avvägningarna och GPS inte är helt jämförbara; bägge tidsperioderna är dessutom för korta för att ge säkra långtidstendenser.

Nyckelord: Island, Reykjanes halvön, Vogarprofilen, precisionshöjdmätningar, nedsjunkning, förkastningsrörelser, modellering av nedsjunkning, Mogi modellen.

Ingrid Anell, Geologiska institutionen, centrum för GeoBiosfärsvetenskap, Lunds universitet, Sölvegatan 12, 223 62 Lund.

1. Introduction

1.1 Thesis project

1.1.1 Introduction to project

Due to its unique geological setting Iceland is an interesting place for the study of crustal deformation. At several locations across the island, precision leveling profiles have been set out. These profiles vary in total length and spacing and consist of permanent benchmarks, set into the bedrock. By measuring the vertical elevation change across the profile over time, it is possible to determine the nature of the surface deformation.

The profiles on the Reykjanes peninsula, southwest Iceland (Fig. 4B), were laid down mostly in the 1960's with the specific intention of studying the rate and nature of the surface deformation within the Reykjanes rift zone (Tryggvason 1974). The study of tectonic plates and their related deformation could on a scientific scale, at the time, be considered new-born. Due to the unique geological setting, Reykjanes was perceived as an excellent place for study, as the rift zone was seen as being the direct continuation of the crest of the mid-Atlantic ridge onto land. Thus, it provided an ideal locality for the study of subaqueous mid-ocean ridge activity, with the benefit of it being on land. The information could then be related to the study of global tectonics, which as mentioned, was an area of growing interest.

The locations for the profiles were selected in areas of obvious recent vertical activity; faults, tilting and fissures. The benchmarks were set in exposed bedrock, which appeared reasonably unaffectable to the action of natural surface processes such as freeze-thaw, or any form of accidental effects. By re-measuring the vertical change between the benchmarks across the profiles over discrete time intervals, it would be possible to determine the nature and effect of subsidence and faulting in the area, and deformation trends occurring within the region. However, with the advent of new technology to measure deformation, such as Global Positioning Satellite (GPS) and Interferometric Synthetic Aperture Radar (InSAR) (Sigmundsson 1997, Gudmundsson *et al.* 2002, Pedersen *et al.* 2003), the older leveling technique for measuring surface deformation in the area, precision leveling, was used less.

One of these profiles is the 4.2 km long Vogar profile (Fig. 6), crossing a fissure swarm in southwest Iceland (Fig. 4C). The latest measurements of the Vogar profile were made in 1976. Hence, the idea behind this thesis was to re-measure the profile, to compare new and old data and to determine what, if anything, has happened since then.

1.1.2 Aims of project

The major aims of the project are:

- Study subsidence within a rift zone
- Examine the nature of subsidence in the area and determine if subsidence is toward the central axis of the plate boundary, affected by a regional component, or confined within the fissure swarm, affected only by this local component.
- Determine the rate of subsidence across the profile and analyze variations in rate over time.

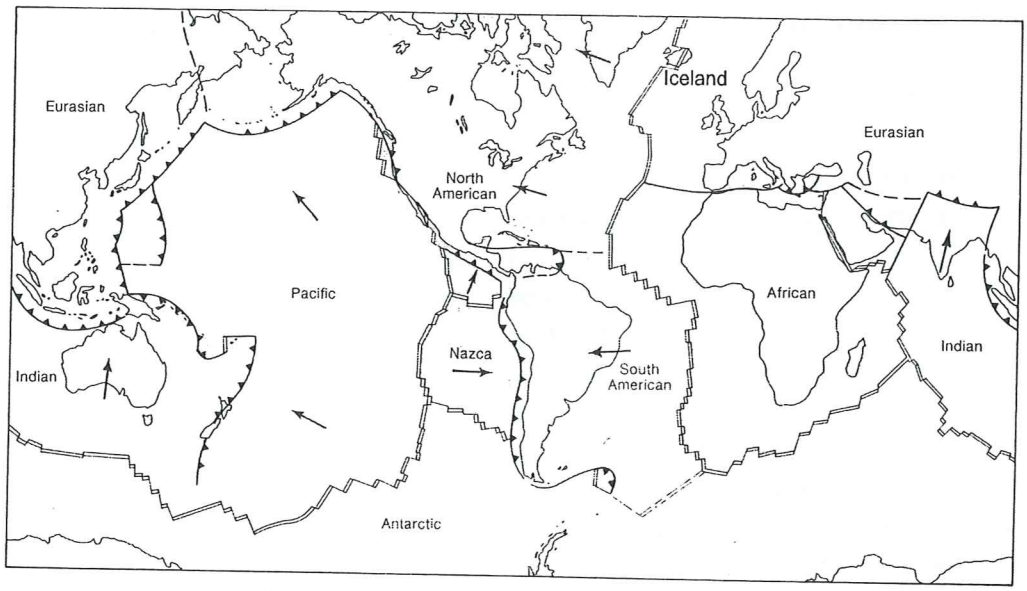

Fig. 1. Map of the world showing the major tectonic plates and the location of Iceland. (Adapted from Dennis 1987)

- Study any eventual fault movement and if present, relate to earthquake activity or progressive movement on fault traces.
- Relate annual subsidence to a model of a line-source of pressure decrease to infer whether it can be fitted to the predicted model of subsidence.

1.2 Geology of Iceland

1.2.1 Plate tectonics

Geology made its appearance in the scientific world in the 18th century into a midst of religious and moral debate. Geological data, chiefly sedimentary and paleontological, appeared early on to question such fundamental beliefs as whether the world was perhaps more than some 4000 years old. If these first sketchy ideas presented rattled the foundations of the beliefs of the time, then when the ensuing ideas pertaining to continental drift and theories of a changing earth were entertained, they certainly brought some of the pillars of assumed knowledge tumbling down. It wasn't however until the mid to late 20th century that concrete answers, and new foundations, were finally presented in this debate. Magnetic anomaly observations of the sea-floor ascertained the mirror image imprints of pole-reversals on opposite sides of the mid-ocean ridges. This finally concluded that the Earth's crust was slowly being pulled apart at places, and also destroyed at others, in the giant global jigsaw puzzle we today know as plate tectonics (Fig. 1).

Plate tectonics was a milestone in the understanding of the evolution of the Earth. The early ideas presented, which gradually evolved into a comprehensive theory, made leeway in explaining the existence and location of most earthquakes, volcanoes and other related deformation features.

Tectonic plates are giant slabs of near rigid conductive material that comprise the lithosphere, which overlies a deep convective layer. These plates interact as

they move, by subduction and destruction, or perhaps better defined as recycling, at destructive plate margins, and accretion at constructive plate boundaries, where the plates move apart. A third type of plate boundary is the conservative plate boundary, where two plates slide against one another along a transform fault.

1.2.2 General geology of Iceland

Iceland has a complex and relatively unique geological setting due to the fact that at this location the mid-Atlantic spreading ridge is superimposed on a deeply rooted hot spot. The hot spot volcanic activity is responsible for building up the excessive igneous foundations that result in Iceland's existence.

The mid-ocean ridge systems consist of roughly 60000km of interactions of faults and active spreading segments. Various forces push or pull apart tectonic plates and new oceanic crust is formed as magma rises to fill in the gaps. Iceland overlies the mid-Atlantic spreading ridge, where the North American and the Eurasian plates are moving away from each other at a spreading rate that averages 1cm/year. Iceland is the only island in the world, which extends well across a whole ridge, allowing for surface observations of spreading processes. Due to the influence of the hotspot activity however, Iceland has an unusual crustal structure and naturally a higher elevation, and hence processes are prone to be similar, but not accurately representative, of those on the sea floor.

Because of the hot spot activity and crustal characteristics, Iceland does not provide us with an exact replica of the relatively simple characteristic spreading centers and transform faults that typify mid-ocean ridges. The plate boundary moves progressively westward with respect to the hot spot, which results in eastward 'jumps' of the spreading

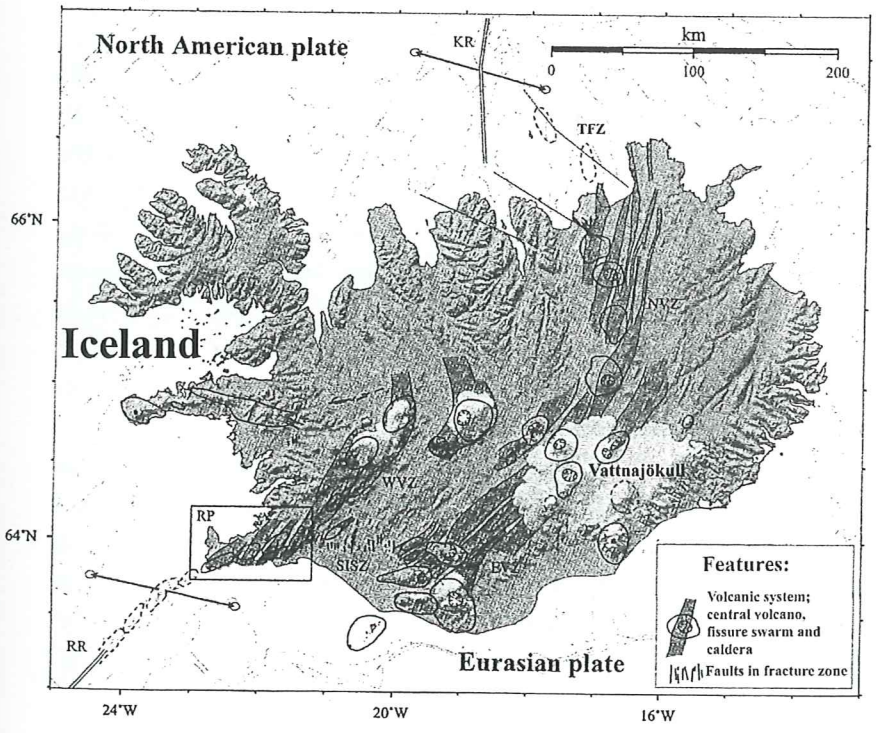

Fig.. 2. Map of Iceland showing main geological features. KR= Kolbeinsey ridge, TFZ= Tjörnes Fracture Zone, NVZ= Northern Volcanic Zone, EVZ= Eastern Volcanic Zone, WVZ= Western Volcanic Zone, SISZ= South Iceland Seismic Zone, RP= Reykjanes Peninsula, RR=Reykjanes Ridge. Arrows indicate direction of plate movement. (Adapted from Hreinsdóttir *et al.* 2001.)

segments. This, as is a common consequence in similar settings, results in parallel spreading zones, sometimes, being active concurrently. At present the hotspot is located beneath Iceland's largest ice-cap, Vattnajökull, is Southeast Iceland (Fig 2).

The mid-Atlantic ridge connects with Iceland at the Reykjanes Peninsula, at the southwestern tip of Iceland, through the Reykjanes Ridge (RR; Fig. 2). The Reykjanes peninsula is an oblique spreading zone (≈SW-NE), characterized by surface fractures, subsided grabens, eruption fissures and ridges of volcanic tuff and breccia (Tryggvason, 1968). This oblique spreading zone connects with the Hengill triple junction, connecting Reykjanes, the Western Volcanic Zone (WVZ) and the South Iceland Seismic Zone (SISZ). This seismic zone has developed as a consequence of the unstable situation arising from, the apparent ridge jump in progress, where the Eastern Volcanic Zone (EVZ) is replacing the WVZ. The SISZ connects the two. The EVZ merges with the Northern Volcanic Zone (NVZ) which in turn gives way to the Tjörnes Fracture zone (TFZ). The TFZ is a seismically active transform zone, connecting the NVZ to the Kolbeinsey Ridge (Fig. 2). The volcanic zones are characterized by volcanic systems with a central volcano and a transecting fissure swarm arranged sub parallel or en-echelon within the volcanic zone (Fig. 2).

1.2.3 The Reykjanes Peninsula

The Reykjanes Peninsula (Fig. 4B), which is the area considered in this project, is a zone of high seismicity and relatively recent volcanism, connecting the Reykjanes ridge to the WVZ and the SISZ (Einarsson 1991). The seismicity is caused by deformation of the brittle crust over a deep aseismic deformation zone (Einarsson 1991). The peninsula is very young, most of it has formed after 0.7Ma (Hreinsdóttir 1998).

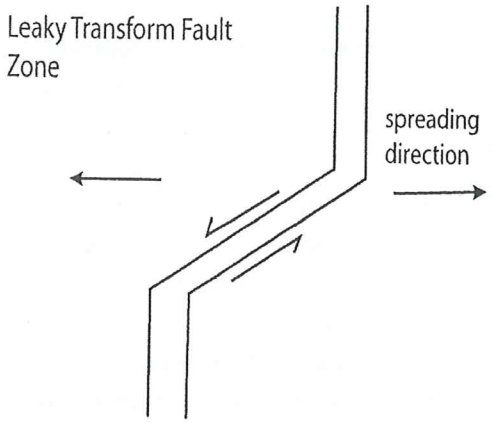

Fig. 3. A simple diagram of a leaky transform fault zone, which characterizes the rift zone on the Reykjanes Peninsula.

The Reykjanes rift across the Peninsula can be termed a 'leaky' transform fault zone (Fig. 3), since the central axis of the plate boundary is oblique, at 30° (Clifton and Schlische 2003), to the spreading direction. Given this setting it is apparent that the boundary on the peninsula encompasses both transform and ridge segment characteristics, i.e. both extension and shear (Clifton *et al.* 2003). Observations have shown that the Peninsula appears to experience two different forms of activity. Periods of rifting, with volcanic eruptions and fissuring occur, followed by seismically active, but volcanically inactive periods (Einarsson and Björnsson 1992).

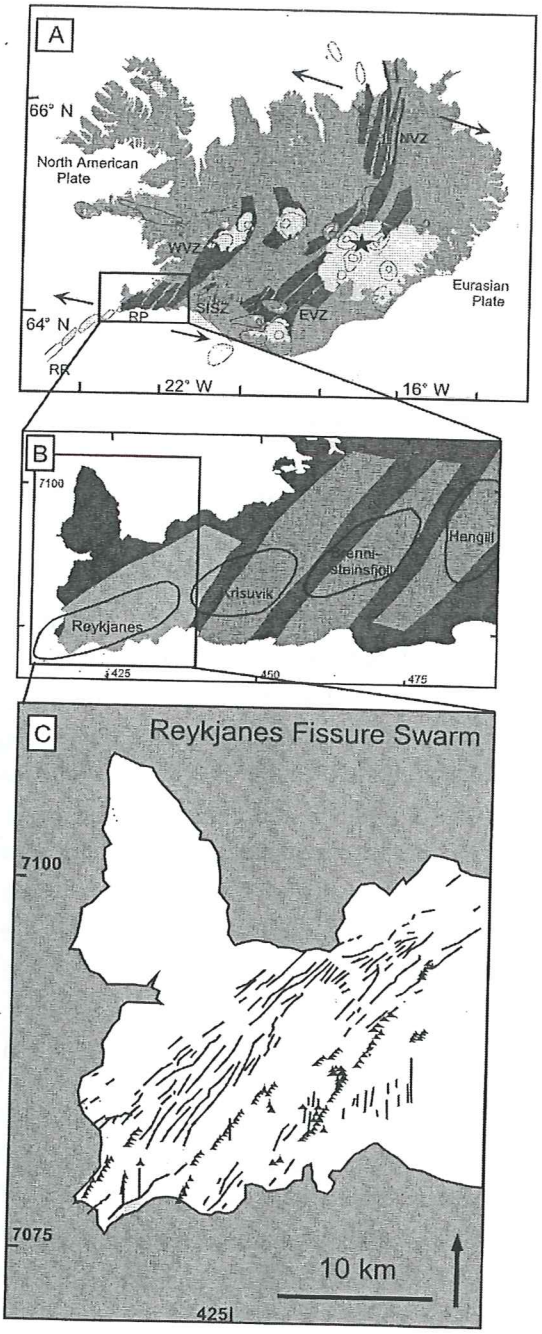

Fig. 4 A) Map showing geometry of ridge segments, RP=Reykjanes Peninsula. Arrows indicate the direction of plate motion. The star shows the present location of hot spot. B) The Reykjanes Peninsula, lighter grey areas indicate volcanic systems including fissure swarms. C) Reykjanes fissure swarm. (Modified from Clifton and Schlische 2003.)

The central axis of the plate boundary has been revealed through seismic data from detailed studies to be between 2-5km wide. It trends 75° across the length of the peninsula (Klein *et al.* 1973, 1977). Earthquake foci are generally found within 1-5km of the surface (Clifton and Schlische 2003).

The area is thought to have become tectonically active through a large rift-jump from the Snæfellsnes rift zone, occurring some 6.5-7.0 million years ago (Sæmundsson 1978, Jóhannesson 1980). Eruptions occurred along fissures, which are generally spread ca 5km apart, striking on average 40° (Clifton and Schlische 2003). These eruptions occurred in four separate volcanic systems (Fig. 4B), Reykjanes, Krìsuvìk, Brenni-steinsfjöll and Hengill, with their own magma supply and distinct fracture groups (fissure swarms). These fissure swarms comprise shear fractures, extension fractures and hybrid fractures (encompassing elements of both types of fracture). NE-trending craters and ridges, from these eruptions, dominate the topography. The regions of highest volcanic activity and production are mainly confined to areas close to the narrow plate boundary (Clifton and Schlische 2003).

1.2.4 Reykjanes stress regime and resulting features

The minimum compressive stress in the region is consistently horizontally oriented in a NW direction. The maximum stress, however, rotates between vertical, causing NE-striking normal faulting (Fig. 5a), and NE horizontal, causing strike-slip (Fig. 5c) on north or east striking faults (Einarsson 1991). The eruptive fissures at the surface open up against the minimum stress,

resulting in dikes (striking NE). Strain release varies in the area from predominantly normal faulting and earthquake swarms in the west toward strike-slip and mainshock-aftershock sequences earthquakes in the east. Recent studies reveal that left lateral shear is at present accumulating on the Peninsula (Sturkell *et al.* 1994, Hreinsdóttir *et al.* 2001).

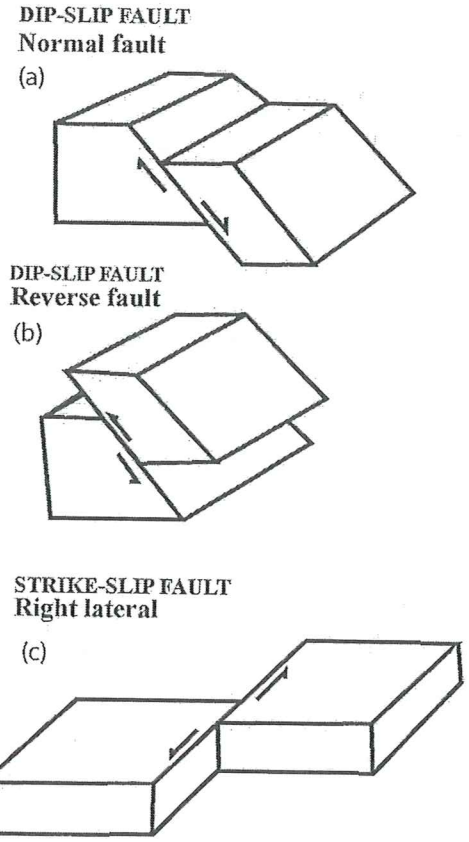

Fig. 5 a) Simplified diagram of normal faulting. B) Simplified diagram of reverse faulting. c) Simplified diagram of right lateral strike-slip faulting

The surface features are compatible with horizontal extension in a NW-SE direction. The grabens in the area are bounded by normal faults, often angled at 60° to the surface, meeting in a deep-seated v-shape at approximately 5km. Below this depth the faults are probably vertical and fill with magma upon widening (Einarsson 1991)

The area is subsiding, i.e. gradually sinking. This is the result of the oblique transform fault zone running along the length of the Reykjanes rift zone. As the plates progressively move further and further apart, the 'leaky' transform zone is subject to extension. This tensional component results in a steady subsidence of the land. Had the system been in equilibrium, we would of course have seen a magma influx from below, to fill the depression which has formed. Volcanic activity has not been noticeable in the area since 1240 AD (Jóhannesson and Einarsson 1998). Offshore eruptions are however more common, with five documented ones since 1550, the latest one in 1926 (Guðmundsson and Sæmundsson 1980).

The geological history of the area appears to encompass periodic events, alternating between volcanically and seismically active periods. These periods in themselves can also be termed episodic as larger seismic events tend to occur in swarms, several years apart.

1.2.5 Geology of Vogar

The Vogar profile is located on old postglacial lava, thought to be around 12500 years old (Sæmundsson 1995). It runs across a zone of intense faulting (fissure swarm). The lava erupted from a shield volcano, Thráinsskjoldur, presumed

active in early postglacial times. The slope on the flanks of the volcano is measured to be 0.05 radians and decreases to 0.02 radians in the vicinity of the profile (Tryggvason 1970).

The fractures in the area (Fig. 16), which amount to several hundreds within the Thráinsskjoldur lava, exhibit a range of strikes, with a clear high frequency between 50°-60° (Clifton and Schlische, 2003). The graben structure is asymmetric. The faults on the northwestern end are subvertical and dip towards the southeast. Further towards the southeast the faults are northwest dipping, facing away from the center of the rift zone.

Table 1. Faults along the Vogar profile

Fault	Benchmarks	Vertical displacement (m)	Dip Orientation
Fault 1	108-111	14	SE
Fault 2	114-115	2	SE
Fault 3	115-116	1	NW
Fault 4	118-119	2	NW
Fault 5	123-124	3	NW
Fault 6	129-130	7	NW
Fault 7	133-134	1.5	NW
Fault 8	142-143	6	NW
Fault 9	147-148	7	NW

2. The Vogar leveling profile

2.1 The profile

The Vogar leveling profile (Appendix 1) runs as a nearly straight line, from close to the village of Vogar near the north shore of the Reykjanes peninsula. It extends inland some 4200 meters, at an azimuth of approximately 155° (Fig. 6). The profile consists of 54 permanent benchmarks, marked 101-154. They lie along a relatively straight profile almost perpendicular to the faults and fissures of the area. The benchmarks are set between 11 and 133m apart, averaging ca 80m. The profile crosses nine normal faults (Fig. 6) showing a vertical displacement between 1 and 14 meters (Table 1) along with a large number of extensional fissures. The fault blocks between faults have been tilted.

The profile crosses the Reykjanes fissure swarm, which extends from near the tip of the southwest shore of the Reykjanes Peninsula in a northeasterly direction narrowing slightly towards the northern shore (Fig. 4B). This fissure swarm, like the others on the peninsula, consists of a graben structure with many open fissures bounded by normal faults (Fig. 14).

Few fissures are located in the areas between the fissure swarms. The Vogar leveling profile extends across almost the whole of the Reykjanes fissure swarm. The last benchmark is located some 400m further on from the easternmost distinct fault along the strike of the profile.

2.2 Method and equipment

Precision leveling is done using two graduated invar rods and a level (Sigmundsson 1996). Invar is a metal alloy which is not appreciably affected by thermal expansion, and hence temperature differences will not affect the measurements substantially; therefore deviations are kept at a minimum. The

level is an apparatus designed to measure very precisely, using laser technology, a height value on each invar rod, from which the elevation difference between the two is calculated.

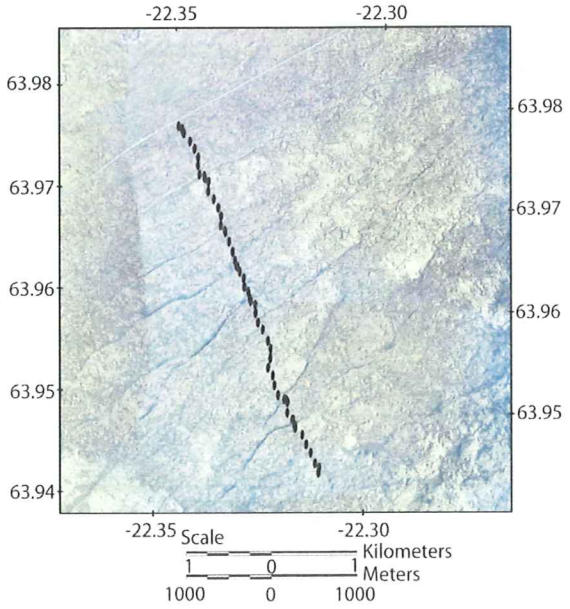

Figure 6. Map showing the location of the 54 benchmarks along the Vogar profile (Appendix 1)

To maximize accuracy the following procedure is used. The rods are placed upright in a vertical position, on two consecutive separate benchmarks, facing the level, which is placed at equal distance from the two rods (Fig. 7). The distance between a rod and level should preferably not exceed 25m. The level is pointed at the first rod and a vertical elevation measurement is recorded. The level is then pointed toward the second rod and two measurements are recorded. The level is finally returned to face the first rod and a second measurement is taken on this rod. Then, while in the field these values are quickly subtracted from each other to get an elevation difference. If the two values differ by more than 0.2mm, the measurements are repeated. A section of the profile is measured in this way, i.e. several benchmarks. The rods are then switched, and the profile is measured back the same distance in the same fashion. This is done to ensure that any inherent error in the rods is cancelled.

When the permanent benchmarks are separated by more than 50m, extra benchmarks are used. These are mobile and placed between permanent markers and used in the same fashion as the permanent benchmarks. When calculating the data the total vertical elevation is determined by summing the separately determined elevation increments to give the vertical change between two permanent markers.

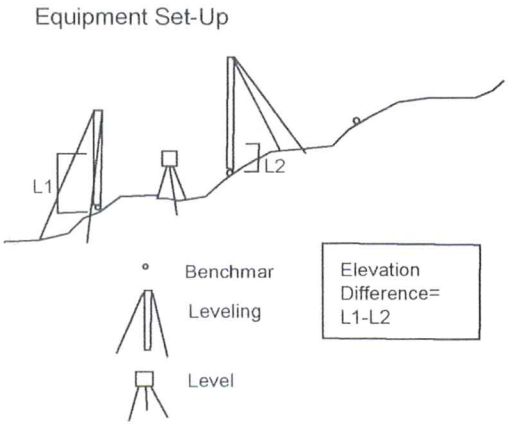

Figure 7. Simple diagram of equipment set up, (interpreted from figure by Sigmundsson 1996).

2.3 Uncertainties from leveling, error calculations

The accuracy for precision leveling ranges from $0.2\sqrt{L}$ mm, where 'L' is in km, for highest order modern leveling to $6\sqrt{L}$ mm,

for lowest accuracy geodetic measurements (Tryggvason 1968, Sigmundsson 1996). Due to random errors in leveling, the standard deviation is proportional to the square root of the distance along the leveling line (Sigmundsson 1996). The square root in the formula means the same error result is obtained for any cumulative distance calculations, as is obtained when summing errors for individual distances using the formula: $\sqrt{(\sigma_1^2 + \sigma_2^2 + ...)}$, where σ is any one individual error. To obtain the highest accuracy one should use invar scale rods and measure the leveling line both forwards and backwards. This method was used for the Vogar leveling 2004 data (Appendix 1), hence the accuracy of the values is within $0.2\sqrt{L}$ mm (eq. 1). The total length of the measured profile, between each benchmark, permanent and non permanent, and via the level, is 4818m, which gives an uncertainty of ±0.439mm between benchmark 101 and 154 (Appendix 4).

2.4 Previous measurements, results and conclusions

The Vogar profile was initially leveled in June 1966, and the measurements were repeated in 1968, 1969 (only part of the profile), 1971 and 1976. The results of these levelings have been reported in several papers (Tryggvason 1968, 1970, 1974, 1981, 1982). In 1966, 1968 and 1971, measurements were made from benchmark 100, which due to road construction has been destroyed. The value for 100-101 from these years was subtracted from each measurement so that all results could be compared within the same reference frame (Appendix 3), since the measurements from 1969, 1976 and 2004 are measured and calculated relative to benchmark 101.

The main observations (Fig. 8, 9, 10) reported from 1966-1976 are summed below as reported by Eysteinn Tryggvason (1968, 1970, 1974, 1981, 1982).

Between 1966 and 1968, a vertical displacement of 6.8mm occurred on the fault between benchmarks 108 and 111 and the whole area was tilted (Tryggvason 1968).

No tilting was observed between 1968 and 1969. The area around the displaced fault 108-111 was uplifted after the fault movement. The hypothetical reason for this is that either the faulting in 1967 changed the permeability of the fault zone leading to changes in the flow of groundwater, which allowed warm water at depth to flow upward, which resulted in a temperature increase and a thermal expansion. Another possible explanation is that the earthquake swarm of 1967 left the fault zone with abnormally low pressures at depth and the magnitude 6 earthquake in 1968 partly reversed the process (Tryggvason 1970).

From 1968-1971 the main deformation observed was a continued regional tilting toward the SE and some minor fault displacement (Tryggvason 1981).

Between 1971 and 1976 the southeastern end of profile subsided 30mm relative to northwestern end. Vertical displacement on two faults (129-130 and 141-143) of ca 20mm each, one in reverse (Fig. 5b) to its otherwise normal displacement occurred. Minor movements on five faults of 2-4mm were observed, most of these had shown indications of minor movements in the earlier measurements (Tryggvason 1981).

Fig.8 (a,b,c) Vertical Elevation Profile

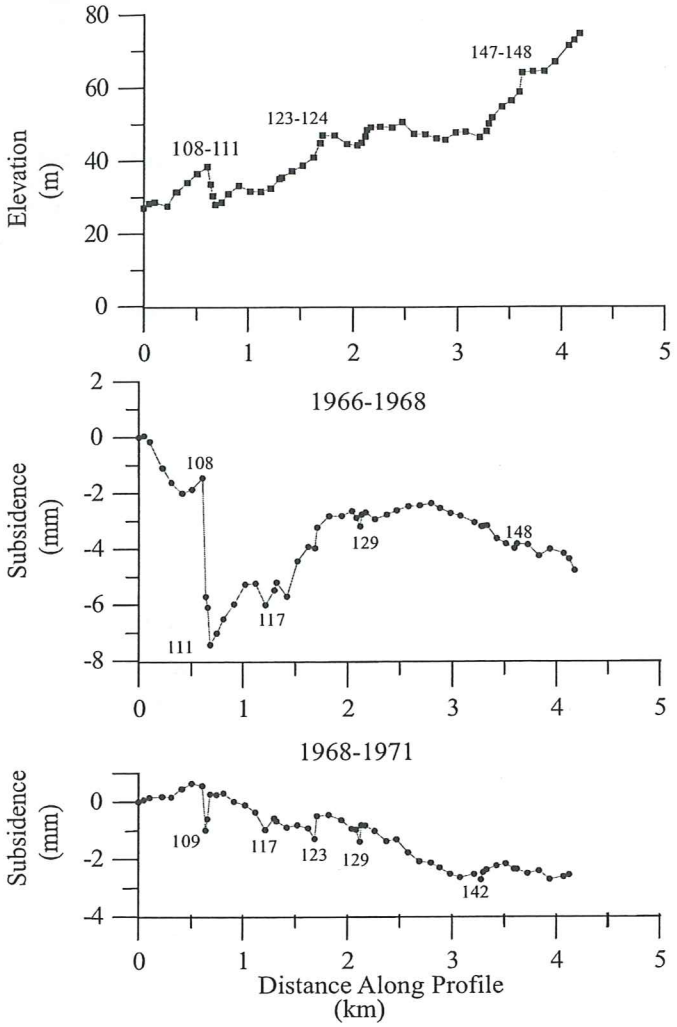

Fig.10(a,b,c) Vertical Elevation Profile

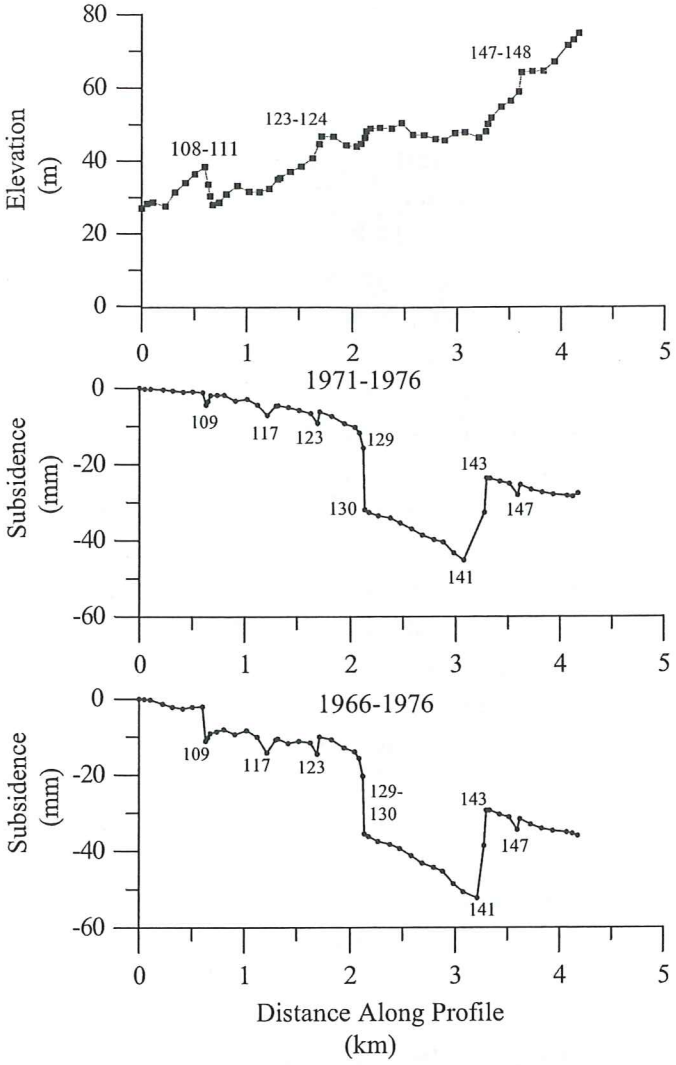

Fig. 9 (a,b,c) Vertical Elevation Profile

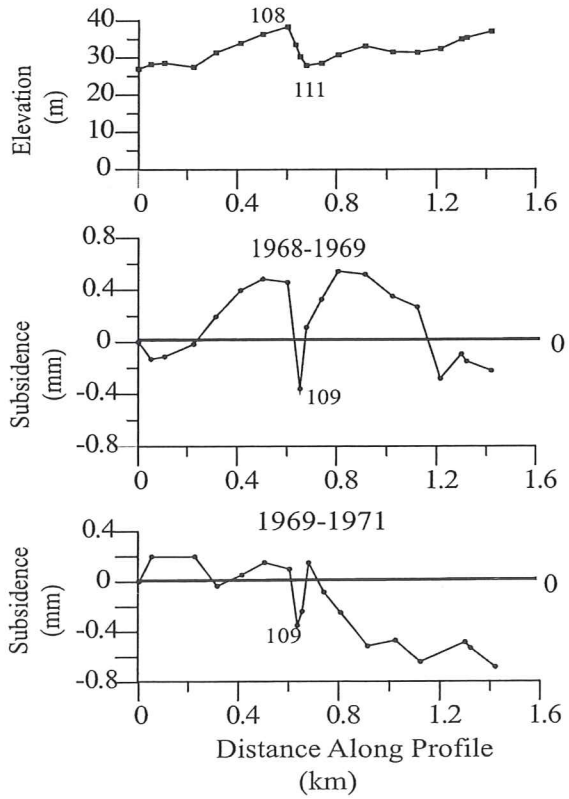

Fig. 8, 9, 10 (a,b,c). Plots of previous observations of vertical change along the profile. Figures (a) show the vertical elevation along the profile. Vertical scale for subsidence values varies between figures 8 b, c, 9 b, c, and 10 b, c, depending on amount of vertical variation during the time-period, but is the same for figures b and c for each figure. Horizontal scale is different for figure 9 because only part of the profile was measured in 1969. 1966-1976 shows a plot of the total vertical change to have occurred between the first and latest of the previous measurments.

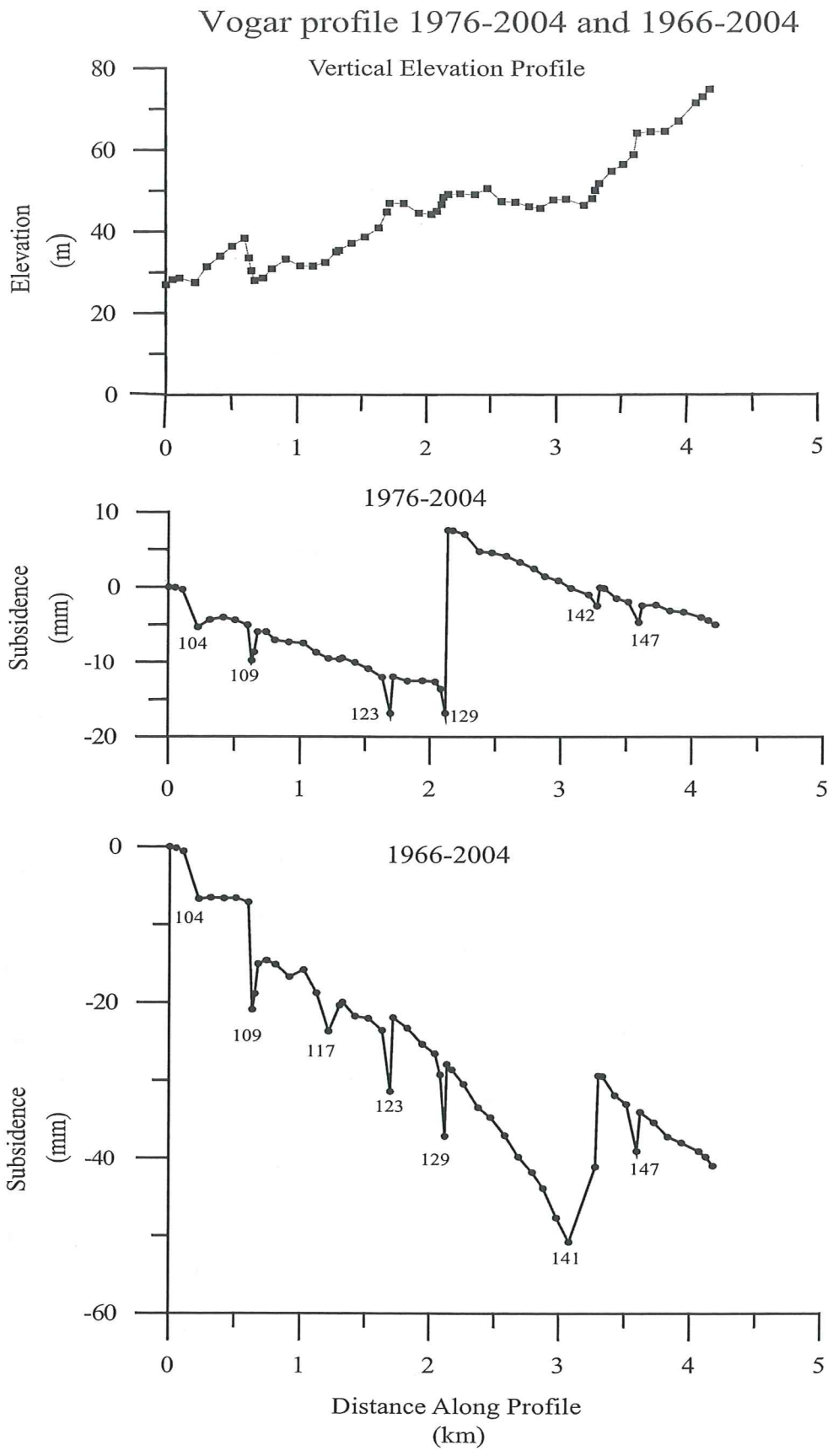

Fig. 11 (a,b,c). a) Vertical elevation profile of the Vogar profile. b,c) Plots of the Vogar Profile 1976-2004 and 1966-2004, showing all subsidence since latest measurements and showing total subsidence since first measurements respectively.

3. Results: Crustal deformation inferred from observations on the Vogar profile 2004

3.1 Subsidence

3.1.1 Vogar data 2004

The Vogar data in 2004 (Appendix 1) was collected over a four day consecutive time period, from the 7th to the 10th May, 2004. For each section between two benchmarks a minimum of four vertical elevation difference values were obtained, two during the forward measurement, and two on the return run. If either measurement in one direction had a discrepancy of more than 0.2mm the measurement was repeated. The mean value for the forward run and the return run were obtained separately and then a mean value for these two was taken and used as the final value. No measurements were disregarded. The difference between the two measurements for each run and the difference between the forward and return values were calculated. This difference between forward and return varied from 0.0 to 0.75mm. The highest discrepancies were often caused by accumulative discrepancies when using several extra benchmarks, when the distance between permanent benchmarks exceeded 50m.

Using the accumulated elevation along the Vogar profile 2004 data and subtracting each accumulated value for another dataset (Appendix 3), one can obtain datasets and plot the change in vertical elevation across the profile. However, it is important to bear in mind that since the values are accumulated, all values previous to a point affect its value, i.e. one erroneous measurement affects all succeeding points with the same error. The error increases with distance as errors should tend to accumulate rather than to cancel.

3.1.2 Subsidence in relation to the central axis of the plate boundary

Examining subsidence along the profile, using the first measurements from 1966 and the measurements in 2004 (Fig. 11c), it is apparent that the area is subsiding. This subsidence can only be represented relative to the benchmark 101. So the data is used to determine the relative change over time, along the length of the profile. Given the tectonic setting it is hypothesized that subsidence in the area should either be at a maximum along the trace of the central axis of the plate boundary across the Reykjanes peninsula, decreasing steadily away from it or alternatively at a maximum at the center of the separate fissure swarms.

If there is a maximum at the center of the fissure swarm, relative subsidence data should reveal a clear maximum along the local Vogar profile, in simple terms, it forms a complete curve. If, on the other hand, the subsidence is at a maximum along the trace of the central axis of the plate boundary we should see an increasing subsidence toward the southeastern end of the profile, simply put, a part of a curve. Because the Vogar profile is aligned across a fissure swarm, and almost perfectly perpendicular to the trace of the Reykjanes rift, it is the ideal place to provide an answer to this question.

Inspecting subsidence plots over different time intervals (Fig. 8, 9, 10, 11), it is evident that the southeastern end of the profile is

Table 2. Average annual subsidence for six benchmarks along the profile during different time periods.

Benchmark	109	118	127	136	145	154
Period	Average annual subsidence (mm)	Average annual subsidence (mm)	Average annual subsidence (mm)	Average annual subsidence (mm)	Average annual subsidence (mm)	Average annual subsidence (mm)
66-68	-2.86±0.09	-2.74±0.12	-1.33±0.15	-1.23±0.18	-1.82±0.20	-2.40±0.22
68-69	-0.64±0.18	-0.10±0.25	*No data*	*No data*	*No data*	*No data*
69-71	-0.12±0.09	-0.16±0.12	*No data*	*No data*	*No data*	*No data*
68-71	-0.33±0.06	-0.19±0.08	-0.32±0.10	-0.70±0.12	-0.75±0.13	-1.18±0.15
71-76	-0.88±0.04	-0.94±0.05	-2.06±0.06	-7.73±0.07	-4.90±0.08	-5.53±0.09
76-04	-0.35±0.01	-0.34±0.01	-0.45±0.01	0.12±0.01	-0.05±0.01	-0.18±0.02
66-04	-0.55±0.01	-0.5±0.01	-0.70±0.01	-1.05±0.01	-0.84±0.01	-1.08±0.01

subsiding at a greater rate than its northwestern counterpart (Fig. 12).

However, also apparent in the 1966-2004 plot is that the central part of the fissure swarm has subsided due to fault movements on two of the main boundary faults near the edge of the fissure swarm. A logical explanation for this observation is that the profile is subject to the effects of both the regional and the local component.

3.1.3 Annual rates of subsidence

Annual rates of relative subsidence are calculated by dividing the difference between two accumulated datasets by the number of years between them. Naturally it is not implied that all movement takes place at a constant rate over each time period, certainly most movements, particularly larger fault movements, occur as discrete events. This rate is only deduced from a very short period of time, the longest period being 38 years. One cannot claim to confirm any hypotheses pertaining to the whole 12500 years since the lava in the area formed. The tendency however, for a given time period, should be ascertainable.

Some aspects of the southeastern end of the profile are immediately noticeable (Fig. 12). Primarily we note that the data from 1971-1976 and 1966-1968 show larger subsidence than the others for benchmark 154, and average of 5.5 mm/yr and 2.4 mm/yr respectively (Table 2).

The data for 1968-1971 and the overall data, 1966-2004, show a similar annual subsidence of benchmark 154 of 1.18 and 1.08 mm/yr respectively. The average annual subsidence for 1976-2004 is 0.18 mm/yr.

The tendencies across the profile up to benchmark 118 are more similar aside from the period 1966-1968 due to the fault movement on Hrafnagjá and 1971-1976 when the rate of subsidence was higher. The remaining time periods: 1968-1969, 1969-1971, (1968-1971), 1976-2004, and 1966-2004 (Table 2), show similar trends often within 0.3 mm of each other.

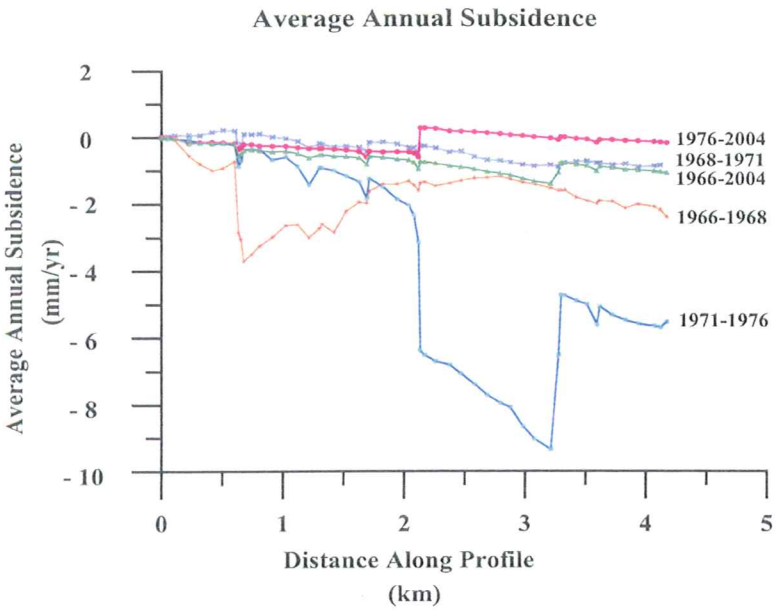

Fig.12. Average annual subsidence along the profile, plotted for all consecutive time-periods when the whole profile was measured.

The regional tilt of the southeastern end of the profile relative to the northwestern end over the 38 year period averages ca 0.25 micro-radians (μrad). The rate was 5 times higher during the period 1971-1976, when the regional tilt component was 1.3 μrad (Tryggvason 1981), and similar in rate to the period 1967-1971 when it was ca 0.22 μrad (Tryggvason 1981).

3.2 Fault movements

3.2.1 Fault movements in the most recent data

The Vogar profile crosses nine faults (Fig. 6) showing varying vertical throw. By plotting the difference in cumulative elevation across the profile for separate time periods, any major fault movement becomes apparent because between benchmarks separated by a fault, a substantial vertical elevation difference appears.

The two most recent datasets are the ones from 1976 and 2004. This plot reveals a relatively even subsidence and tilt along the profile aside from the fault movement at fault 129-130 of 24 mm (Fig. 11c). Along with this movement, minor movements on faults 108-109 (108-111), 123-124 and 147-148 (all $\leq$ 5mm) have occurred. Minor movements on these faults, along with a minor movement at 117-119, also occurred from 1966-1976 (Fig. 10c).

3.2.2 A possible error in the 1976 data

A fault movement along the profile is confirmed if it is apparent from two independent datasets. For example the fault movement on 141-143 seen between 1971 and 1976 is visible also in the 1966-2004 data (Fig.11c). If, however, a fault movement is unconfirmed, then we cannot ascertain if it actually has occurred.

Comparing the measurements from 1976 with the new dataset from 2004 (Fig. 11b), reveals a striking feature: a 24mm normal displacement on the fault between benchmarks 129 and 130, which moves the

section beyond this above benchmark 101. This suggests either an uplift of the area, or a greater relative subsidence of the area preceding the fault including benchmark 101. Also striking is that a reverse movement of ca 16mm on the same fault, apparently occurred between the 1971 and the 1976 measurements.

There are two possible explanations to this observation. The first possibility suggests the following scenario.

- Between 1971-1976 a normal fault movement occurred on fault 141-143 (20mm) and a reverse movement occurred on 129-130 (16mm)
- These movements caused the block between 129-130 and 141-143 to subside as a single unit
- Between 1976 and 2004 the "system" acted to restore equilibrium by normal fault movement meaning:
    1. Either a normal fault movement on 129-130, with all benchmarks prior to this point subsiding as a single block
    2. Or the ground beyond 129-130 was uplifted to balance the reverse movement (Fig.13)

The other possibility is that the movement measured on this fault is due to an erroneous measurement in the 1976 data. Since all movement is measured relative to a single point, and all graphs made are comparing one dataset to another, it is hard to distinguish a single erroneous measurement. Also, one erroneous data affects any data it is compared to. In this instance, a reverse fault movement on 129-130, followed by a normal movement in the consecutive time period, is indistinguishable from a scenario, where no movement occurred at the fault.

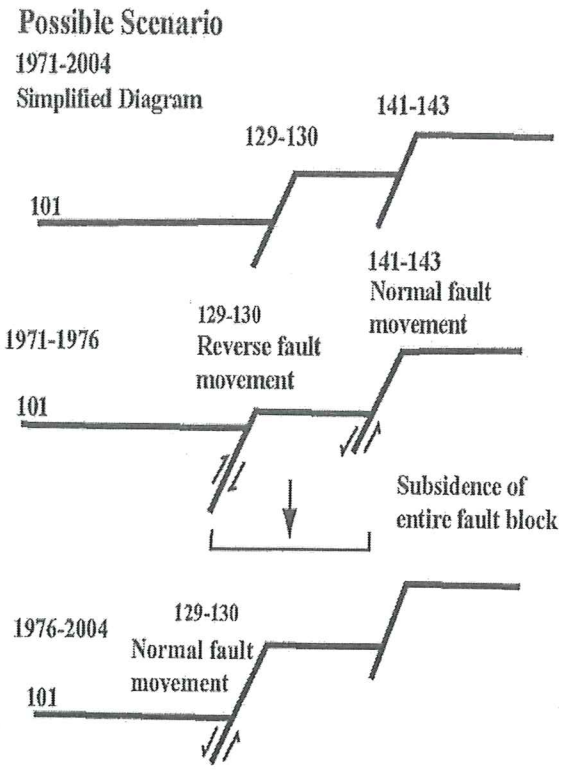

Fig. 13. Simplified diagram of the possible development on faults 129-130 and 141-143 between 1971 and 2004.

Because the measured fault movement on 129-130 is substantial and hence affects both subsidence and fault data, and stemming from the fact that it is unconfirmed, the data will not be used in model calculations. For model calculations we will use only the 1966-2004 dataset. However, because much substantial deformation took place between 1971 and 1976 the data will be taken into account when discussing subsidence and fault movements. The data will mainly be viewed under the assumption that the data

Table 3 – Total and annual fault movement

Fault	Years	66-68 (mm)	68-69 (mm)	69-71 (mm)	68-71 (mm)	71-76 (mm)	76-04 (mm)	66-04 (mm)	Error 2004 (mm) Dip orientation/ faulting orientation 66-04
108-109/ 108-111	Total	-4.26/ -5.98	-1.11/ -0.35	-0.45/ *0.05*	-1.55/ -0.30	-3.24/ -0.72	-4.75/ -0.92	-13.80/ -7.93	±0.07/ 0.09
	Annual	-2.13±0.03/ -2.99±0.04	-1.11±0.07/ -0.35±0.09	-0.15±0.03/ *0.03±0.04*	-0.52±0.02/ -0.10±0.03	-0.65±0.01/ -0.15±0.02	-0.17±0.00 -0.03±0.00	-0.36±0.00 -0.21±0.00	SE/ SE
114-115	Total	*0.71*	-0.17	*0.05*	-0.12	*0.43*	-0.12	*0.90*	± 0.07
	Annual	*0.36±0.04*	-0.17±0.07	*0.02±0.04*	-0.04±0.02	*0.09±0.01*	-0.00±0.00	*0.02±0.00*	SE/ *NW*
115-116	Total	0.04	*-0.08*	*-0.17*	*-0.25*	*-1.49*	*-1.25*	*-2.96*	± 0.06
	Annual	0.02±0.03	*-0.08±0.06*	*-0.06±0.03*	*-0.08±0.02*	*-0.30±0.01*	*-0.05±0.00*	*-0.08±0.00*	NW/*SE*
117-119	Total	0.81	0.13	0.17	0.30	2.54	0.07	3.73	± 0.06
	Annual	0.41±0.03	0.13±0.06	0.09±0.03	0.10±0.02	0.51±0.01	0.00±0.00	0.10±0.00	NW/NW
123-124	Total	0.74	No data	No data	0.81	3.01	4.92	9.47	± 0.03
	Annual	0.37±0.01			0.27±0.01	0.60±0.01	0.18±0.00	0.25±0.00	NW/ NW
129-130	Total	0.42	No data	No data	0.57	*-16.18*	24.44	9.25	± 0.03
	Annual	0.21±0.01			0.19±0.01	*-3.24±0.01*	0.87±0.00	0.24±0.00	NW/ NW
133-134	Total	0.15	No data	No data	0.064	*-1.32*	*-0.16*	*-1.26*	± 0.07
	Annual	0.08±0.03			0.02±0.02	*-0.26±0.01*	*-0.01±0.00*	*-0.03±0.00*	NW/ *SE*
141-143	Total	*-0.137*	No data	No data	0.07	23.03	0.95	23.91	± 0.07
	Annual	*-0.07±0.04*			0.02±0.02	4.61±0.01	0.03±0.00	0.63±0.00	NW/ NW
147-148	Total	0.16	No data	No data	-0.01	2.64	2.25	5.04	± 0.05
	Annual	0.08±0.02			-0.00±0.01	0.53±0.01	0.08±0.00	0.13±0.00	NW/ NW

The annual rate is calculated by dividing the total fault movement by the number of years in the time period. This assumes that fault movement is constant during the time period. Italics indicate movements reverse to that normal on fault. The error is calculated using distance measurements between faults from 2004 with formula described in section 2.3. Errors from previous observations are generally smaller that those from 2004 as $0.15\sqrt{L}$ was used for calculations (Tryggvason 1968). The general consensus today is that $0.2\sqrt{L}$ is the highest accuracy (Sigmundsson 1996) that can be obtained and hence the 2004 error data was set as standard, and no mean error for each two compared data sets was obtained. For annual rates the total error was divided by the number of years for each time period.

Fig. 14. The Vogar graben seen from above. Photographed by Fredrik Holm

Fig. 15 Fault 108-111, Hrafnagjá, the first fault along the profile

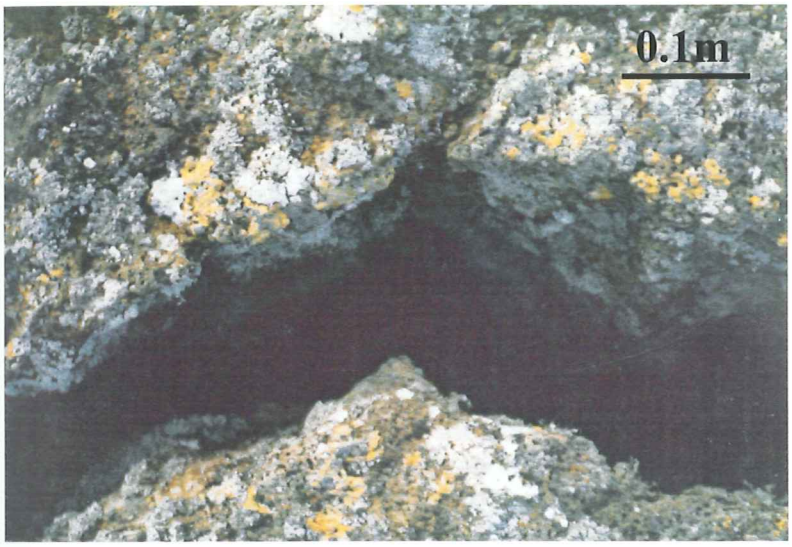

Fig. 16. A ca 20cm wide fracture close to fault 129-130

Fig. 17 Fault 129-130 shows vertical walls with seemingly little vertical displacement.

Fig. 18. Less than 50m westward from Fig. 17 the vertical walls give way to a clear fault scarp. This type of behaviour is visible at most prominent faults.

is in fact correct. However, because the possibility of an erroneous measurement exists, this possibility will be considered in the discussion section.

3.2.3 Total fault movement

The 1966-2004 data shows some form of movement on all the larger faults (Table 3). The largest distinct displacement is seen at fault 141-143, and the second largest on fault 108-111. Fault 108-111 appears active during all time-periods, with some degree of movement perceivable between benchmarks 108-109. Fault movement on 141-143 is almost exclusively confined to the time period 1971-1976.

Faults 117-119, 123-124, 129-130 and 147-148 all show some degree of normal faulting between 4 and 9mm total, over the whole time-period.

Faults 114-115, 115-116 and 133-134 all show reverse fault movements over the whole time period. The movement on the fault is very small at faults 114-115 and 133-134, ca 1mm, and small, 3mm, at fault 115-116.

Between benchmarks 103 and 104 there appears to be a fault movement of ca 6-7mm, which occurred between 1976 and 2004 (Fig. 11b).

3.2.4 Annual rates of faulting and progressive fault movement

We can define progressive faulting as the process by which small movements on a given fault occur fairly often. Along the Vogar profile, they occur as a result of a tensional force. These movements occur sporadically, but sufficiently often to allow repeated movements within a few years. The deduced annual rate can of course not be considered representative given the short time span, but might give an idea of the rates of small scale movements occurring at present. We can obtain and use the average annual rate of the fault movement. This rate can then be correlated to the total movement, which has taken place on the fault since the assumed faulting began, ca 12,500 years ago.

It is apparent that the periods between 1966 to 1968 and 1971 to 1976 were periods of higher activity than periods 1968-1971 and 1976-2004 given their higher rates of annual faulting (Table 4). Looking at these time periods and disregarding the three faults that generally show reverse movements (114-115, 115-116 and 133-134), the time period 1966 to 1968 has rates of faulting on three out of six remaining faults greater than the rate needed for the total vertical throw over 12500 years. From 1971 to 1976 four rates of faulting are close to or higher than the, would be, average rate. The rate of faulting on fault 129-130 is considerable, but during this time-period, it was reverse. Between 1968 and 1969 rates of faulting are significant on two of the faults, including 114-115 which generally shows reverse fault movement.

Aside from single moderately significant fault movements, 123-124 from 1968-1971, and 129-130 and 141-143 from 1976-2004, the other time periods are considerably less active with many cases of apparent reverse, or insignificant movement. The overall rate between 1966 and 2004 has a rate similar to that needed for the total vertical movement on two faults, 123-124 and 141-143. Otherwise the overall rates are less than that needed for the total vertical movement.

Table 4 –Average annual rate of fault movement and projected rate for 12500 years

Fault	Total vertical throw (mm) /orienataion	Annual/ In 12500yrs (mm)	66-68	68-69	69-71	68-71	71-76	76-04	66-04
108-111	14000 SE	Annual	-2.99	-0.35	-0.03	-0.10	-0.15	-0.03	-0.21
		In 12500 yrs	**37400**	4375	313	1250	1810	411	2609
114-115	2000 SE	Annual	*0.36*	-0.17	*0.02*	-0.04	*0.09*	-0.00	*0.02*
		In 12500 yrs	*4450*	**2113**	*196*	509	*1075*	54	*296*
115-116	1000 NW	Annual	0.02	*-0.08*	*-0.06*	*-0.08*	*-0.30*	*-0.05*	*-0.08*
		In 12500 yrs	238	*1050*	*700*	*1054*	*3728*	*563*	*974*
117-119	2000 NW	Annual	0.41	0.13	0.09	0.10	0.51	0.00	0.10
		In 12500 yrs	**5069**	**1613**	1081	1259	**6350**	33	1225
123-124	3000 NW	Annual	0.37	No data	No data	0.27	0.60	0.18	0.25
		In 12500 yrs	**4638**			**3371**	**7513**	2195	**3116**
129-130	7000 NW	Annual	0.21	No data	No data	0.19	*-3.24*	0.87	0.24
		In 12500 yrs	2650			2350	*40450*	**10913**	3043
133-134	1500 NW	Annual	0.08	No data	No data	0.02	*-0.26*	*-0.01*	*-0.03*
		In 12500 yrs	969			266	*3305*	*75*	*415*
141-143	6000 NW	Annual	*-0.07*	No data	No data	0.02	4.60	0.03	0.63
		In 12500 yrs	*863*			300	**57575**	**4250**	**7863**
147-148	7000 NW	Annual	0.08	No data	No data	-0.00	0.53	0.08	0.13
		In 12500 yrs	1013			25	**6588**	1000	1658

Data in italics show movement reverse to normal displacement, this includes hypothesized vertical throw in 12500 years, which is always written as a positive value regardless of orientation of fault movement. Bold numbers indicate significant rates within 75% of the rate needed for total vertical thrown and would, hence, if continuous, result in a vertical displacement almost equal to or greater than the total vertical throw.

4. Earthquake analysis

Earthquakes occur on a rather continuous basis, suggesting that during a few years, one or several substantial events are likely to occur along the Reykjanes rift zone. This is due to the build up of stress along the rift itself. According to Tryggvason's (1968, 1970) analysis of the Vogar profile data from 1966-1968 and 1968-1969, earthquakes are a key factor contributing to fault movement. Previous observations (Tryggvason 1968, 1970, 1981) indicate that the fault movement on Hrafnagjá (fault 108-111) between 1966 and 1968 was due to an earthquake in the vicinity of the profile. The subsequent uplift recorded in the following dataset (1968-1969) could be due to a partial reversal of the movement triggered by another earthquake.

Presumably earthquakes affected faults along the profile also after 1969, meaning it should be possible to relate fault movements observed to significant earthquakes during the related time period. Apparent from our data is that earthquakes can both cause a normal fault movement, a reverse movement or a partial or total reversal of a movement, which was

initially normal or reverse. From 1976-2004 we have an apparent reversal of a reverse movement on fault 129-130. It is aimed here to provide a plausible scenario for this development, along with any apparent trends for other time periods.

4.1 Reference frame

In order to narrow our search a general reference frame was defined (Fig. 19). The South Iceland lowland (SIL) seismic network database, which provides preliminary earthquake locations, only included earthquakes > magnitude 4 prior to 1990, and hence this magnitude was set as the minimum. We selected an area within latitude 22°00'- 22°30' on land on the Reykjanes peninsula. Within this reference frame it was assumed plausible that earthquakes may have effect on the Vogar profile.

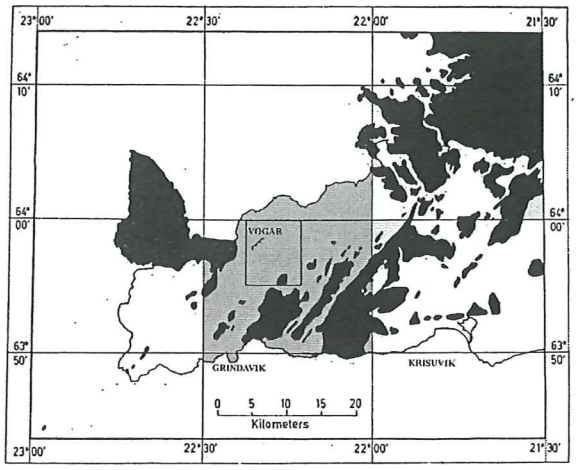

Fig. 19. Map of the general reference frame created for earthquake analysis. The area shaded grey marks the reference frame, the Vogar profile area is marked by a rectangle (Adapted from Tryggvason 1968).

4.2 SIL

Data on major earthquakes (>magnitude 4) was attained from the SIL seismic database. The data is based on manual routine corrections of the automatic bulletin produced by the SIL system and does not provide the most accurate results available. However, given that we are using earthquake data only to define trends of subsidence and faulting in relation to earthquakes and to provide plausible seismic causes for certain events, the absolute magnitude and absolute location are not fundamental.

4.3 Earthquakes prior to 1976

4.3.1 1966-1968

Between 1966 and 1968 six events with magnitude >4 were recorded by the SIL seismic network within the area during the earthquake swarm of 1967. As reported by Tryggvason, one of these could have caused the dip-slip motion on the Hrafnagjá fault (108-111).

4.3.2 1968-1971

In late 1968, after the 1968 data was collected there was a substantial earthquake affecting the area. It occurred just outside the reference frame but with its magnitude, 5.4, it is possible that it caused the partial reversal of the fault movement on Hrafnagjá recorded in the 1969 dataset. Following this, no events were recorded until late 1971, when the 1971 data had already been collected.

4.3.3 1971-1976

We have mentioned this period, along with 1966-1968 to be an 'active' period, simply because movements on faults and the rate

of subsidence had been greater than average over the whole time period. Earthquake data is consistent with this scenario. Within our stated frame of effect we found as many as 25 earthquake events which could have caused a fault movement.

4.4 Earthquakes 1976-2004

4.4.1 Earthquakes within the reference frame

Within the reference frame, between 1976-2004, we find a number of earthquakes (Table 5). Given the long time period however, one cannot consider them many. In fact, between 1976 and 1989 no events occurred at all. This is the result of the apparently rather considerable release of strain during the time period 1971-1976, with 25 earthquake events. GPS geodetic observations across the oblique plate boundary show an accumulation of left lateral shear stress in the period 1986-1992 (Sturkell *et al.* 1994). Two events occurred in 1990 and 2000, respectively, and one in 2003. These events cannot be considered ample for that stress release; hence the only logical conclusion is that stress is still accumulating on the peninsula.

4.4.2 Earthquakes outside of the reference frame

Two large earthquakes occurred in the SISZ on June 17th and June 20th in the year 2000. These earthquakes were felt as far as 200km from their epicenters (Stefánsson *et al.* 2000).

According to the Icelandic Meteorological Office (IMO), the two earthquakes have the following preliminary seismological parameters (Stefánsson *et al.* 2000):

- 2000-06-17 15:40 63.97°N 20.37°W, depth: 6.3 km. Moment magnitude 6.5
- 2000-06-20 00:51 63.98°N 20.71°W, depth 5.1 km. Moment magnitude 6.4

Table 5. Earthquakes in our defined reference frame 1976-2004

Date Time	Lat/long	Local magnitude	Depth (km)
1990-03-19 10:46	*64.0 -21.9*	*4.7*	*2*
1990-03-19 10:48	*64.0 -21.9*	*4.0*	*8*
2000-06-17 15:45	63.9 -22.0	4.4	4.7
2000-06-17 15:45	63.9 –22.1	4.6	2.8
2003-08-23 02:00	63.9 -22.1	4.3	4.1

Italics indicate events just outside of the stated reference frame, but close enough to warrant attention.

Two earthquakes occurred within our stated frame five minutes after the large event on June 17th implying that motion was triggered along the plate boundary on the peninsula as a result of the stress release in the SISZ. Along with these two events, the effects of the large earthquakes in the SISZ will almost definitely have been noticeable in the Vogar profile region. Two larger earthquakes of magnitude 5.1 and 5.0, respectively (Clifton *et al.* 2001), also occurred in the vicinity of the Hengill triple junction in 1998.

5. Modeling subsidence

Given the visible influence from the regional component on the profile, it was attempted to relate these observations to a model. The observations and the model could then be related to GPS data collected on the Reykjanes peninsula during an 11 year period. This was done in order to correlate the observed relative subsidence with the absolute value for subsidence.

5.1 The line-source model

Simple models can be used in the study of the rather complex deformation related to plate boundaries. The model we use is based on the Mogi model (Mogi 1958). By studying vertical surface deformation at volcanoes, Mogi derived a model to relate surface deformation to subsurface pressure change of a spherical source.

5.1.1 Model and derivation

We used a simple model to interpret our subsidence results. The model source is a line-source of pressure decrease within an elastic half space. The line-source model for surface subsidence is obtained by integration of the Mogi model which is a model for point source calculations. This model is based on material loss beneath the locking depth (d_{lock}). Below the locking depth plate movements are accommodated by ductile deformation which is not balanced by influx of new material from underneath, causing subsidence along the plate boundary (Vadon and Sigmundsson 1997). The location of the line-source is set at the locking depth beneath the plate boundary. A simplification of the model was that the radius of the spherical source was small compared to its depth, making it equivalent to a point source. Using elasticity theory this model describes the vertical and horizontal deformation components caused by a point source of pressure (Mogi 1958).

5.1.2 Equation and terms

The equation used for calculations of the subsidence was the following

$$\upsilon_{vertical} = h_{rift}\, d_{lock}^{2}(d_{lock}^{2} + y^{2})^{-1} \quad \text{(eq. 2; Vadon and Sigmundsson 1997)}$$

Where $\upsilon_{vertical}$ is the vertical displacement (subsidence) at the location of interest, h_{rift} is the maximum surface subsidence directly above the line-source, d_{lock} is the locking depth and y is the distance from the source of linear pressure decrease, in our case the central axis of the plate boundary.

5.1.3 Parameters

The central axis of the plate boundary is located about 9-11km from benchmark 101. In our calculations we tested 10.5 and 9.5 km as a y-value for benchmark 101. An absolute value is hard to ascertain given that the plate boundary is by no means a single, perfectly located, infinitely thin line. The d_{lock} and h_{rift} parameters were varied within the ranges of values calculated for the area using the same model in another study in the vicinity. The results of this study gave an h_{rift} value of 6.5±1mm/yr and a d_{lock} of 5±1.5km/yr (Vadon and Sigmundsson 1997).

The third parameter that was varied was the annual subsidence of benchmark 101. Since, the results of the profile are only relative to benchmark 101 this value is varied to provide a best fit to the model.

The model describes the assumed effect of the plate boundary on the profile. Because our profile is subject to the effects of both this regional, but also a local component, it was aimed to provide a best-fit with the benchmarks assumed to be affected almost exclusively by the regional component, in this case benchmarks 101-103 and 141-154.

5.1.4 Calculations

Calculations were done separately for the model and the observed data. A model value of subsidence was calculated for each distance representing a benchmark. These distances were not the same as those used when drawing the profile as the model data had to be fitted to a straight line. The actual benchmarks were projected onto a line between benchmarks 101 and 154 extended to the plate boundary. This means that the relative subsidence for the points along the line, is assumed to be the same as that of the point, from which the projection was done.

To determine the fit we used a least squares criterion (Bevington 1969, as quoted by Sturkell and Sigmundsson 2000). The equation used for this calculation is the following:

$$\chi^2 = \sum \left(\frac{\text{Predicted - observed}}{\sigma} \right)^2$$

(eq. 3; Sturkell and Sigmundsson 2000)
'Predicted' are the model values obtained, 'observed' are the Vogar values from 1966-2004. Sigma (σ) is the uncertainty value. A smaller χ^2 value means a better fit.

To determine the degree of fit when comparing graphs with large χ^2 values we used a simpler version of the equation:

$$\text{Fit} = \sum \left(\text{Predicted - observed} \right)^2 \quad \text{(eq. 4)}$$

The same principle applies; smaller values indicate a better fit with the graph.

5.2 1993-2004 GPS data

5.2.1 Brief introduction to GPS work

Across the Reykjanes peninsula there is a network of about 50 GPS points. Starting in 1993, GPS measurements were performed at several of these points. Some new measurements were made in 1995 and almost all points were re-measured in 1998. After the earthquakes in 2000, the GPS points have been measured every year (Hreinsdóttir 1998, 2001). Among the points is the VOGA GPS point, which incidentally corresponds to benchmark 106 of the Vogar leveling profile. This point was measured several times between 1993 and 2004. Along the projected line toward the plate boundary is the NAUF (formerly termed NAUT) GPS point which was measured several times between 1993 and 2003.

5.2.2 GPS data of VOGA and NAUF points

- Results for the VOGA GPS point give an average subsidence rate of -6.7± 3.7 mm over the 11 year period (Þóra Árnadóttir, personal communication 2004).
- Results for the NAUF GPS point from 1993-2003 is -4.7 ± 4mm/yr assuming constant subsidence rate before and after the June 2000 earthquakes. However rates are substantially higher in the time period between 2000 and 2003, -12.5±5mm/yr, and lower,

-4.3±3mm/yr, between 1993 and 1998. (Þóra Árnadóttir, personal communication 2004).

5.3 Modeling

Although the graph for 1966-2004 can be plotted to fit well with the model, this can only be done with a value of subsidence for benchmark 106 of <3mm. Three millimeters is the minimum absolute value obtained from the GPS results. The best-fit obtained was plotting 9.5km from the plate boundary and using an h_{rift} value of 5.5mm/yr and a d_{lock} value of 3.8km (Fig. 20). The χ^2 value was then 0.29. This χ^2 value was calculated using only the benchmarks assumed to be affected by the regional component, i.e. 101-103 and 143-154.

Within the parameters stated for h_{rift} and d_{lock} values the maximum subsidence obtainable for benchmark 106 is 3.05 or 3.85 mm, depending on whether benchmarks 101-103 or 143-154 are set to fit the graph. This is done with h_{rift} 7.5mm/yr and d_{lock} 7.5km and a plate boundary 9.5km away. This plot does not correlate well in a graph (Fig. 21). The χ^2 value for both cases is very high. When comparing the fit of the graphs (eq. 4), the plot when fitting 101-103 had a value of

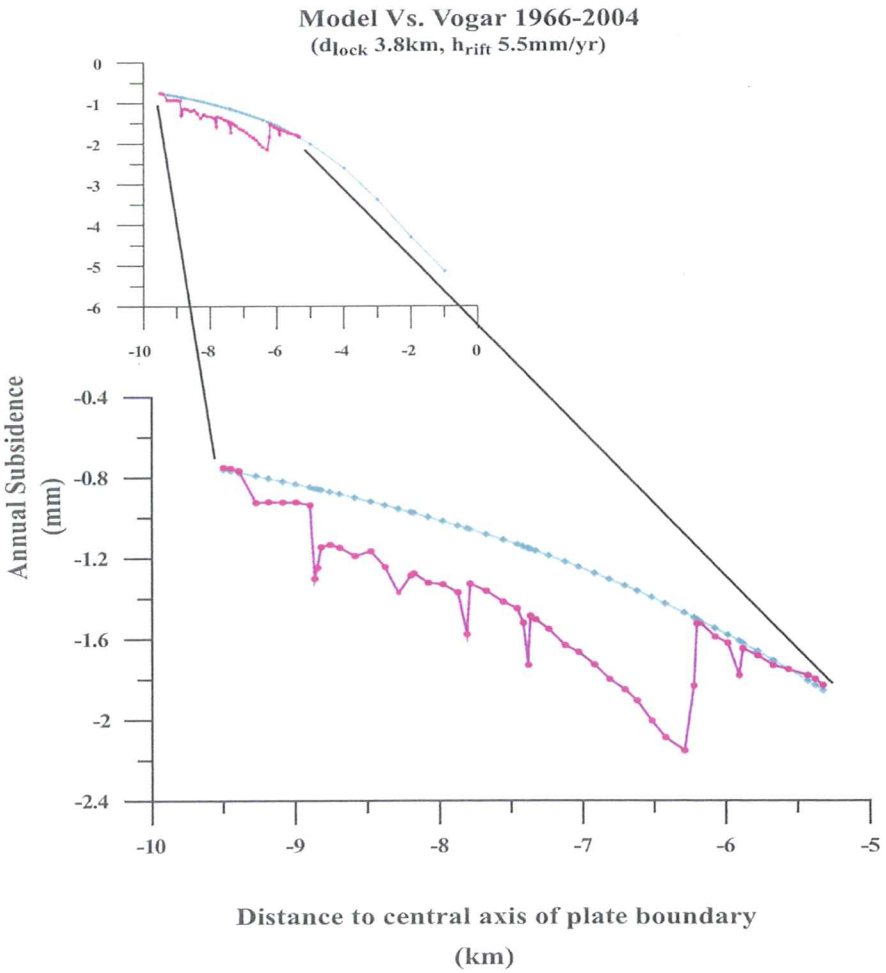

Fig.20. Plot of the best fit of the Model Vs. Vogar data 1966-2004 using d_{lock} 3.8km and h_{rift} 5.5mm/yr and a plate boundary located 9.5km away from the first benchmark.

2.97, the plot when fitting 143-154 had a value of 1.44 as compared to 0.19, which is the value for the best fit with the model.

It is important to take into account the fact that the GPS data reflects subsidence over an 11 year period and our Vogar data encompasses a 38 year period. It is evident when viewing GPS data that rates of vertical deformation vary over time and the error margins are large. In our model, we have assumed that the average for the 11 year period, 1993-2004, is similar to the average for the total 38 year period, 1966-2004

.

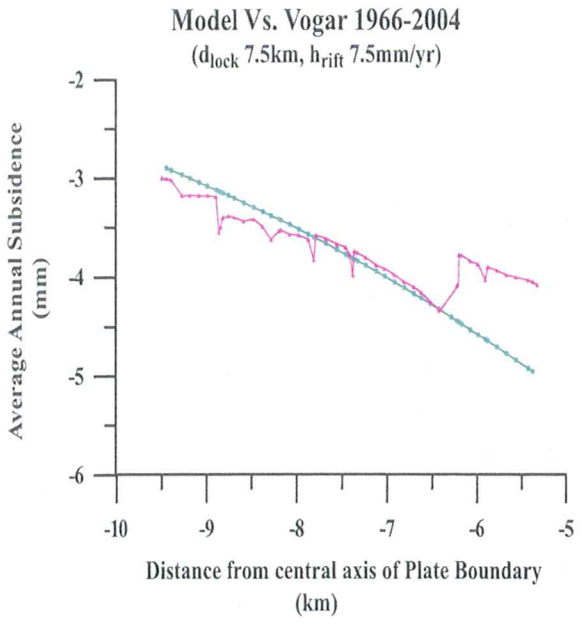

Fig. 21. Plot showing the difficulty in fitting the maximum subsidence obtainable using a model with parameters hrift 7.5 mm/yr and dlock 7.5km to the Vogar data from 1966-2004.

6. Discussion

6.1 Subsidence

6.1.1 General subsidence

Subsidence of the southeastern end of the profile occurs at a higher rate than the northwestern part. This is the result of a regional tilting due to the influence from the central axis of the plate boundary. At the same time it is apparent that subsidence within the local fissure swarm also affects the profile.

The only fault movements to have occurred which cannot be termed "local", i.e. confined to one benchmark on the down-throw side of the fault (see section 6.2.4), are those on faults 108-111 and 141-143, dipping SE and NW, respectively. These fault movements have caused subsidence of the central area of the fissure swarm (benchmarks 109-141). Benchmarks 104-108 have slid down as a block, also seemingly an effect of the local fissure swarm.

These observations imply that the profile is subject to the effects of both the regional subsidence component at the plate boundary, along with the more local effects of the tensional regime within the fissure swarm. Benchmarks 101-103 and 143-154 appear affected only by the regional component, while the regional effect on benchmarks between them has been locally overprinted.

6.1.2 Annual rates of subsidence

1966 to 1968 and 1971 to 1976 show the highest rates of annual subsidence, 5.5 and 2.4mm/yr respectively (Fig. 12). This is a consequence of the fault movements

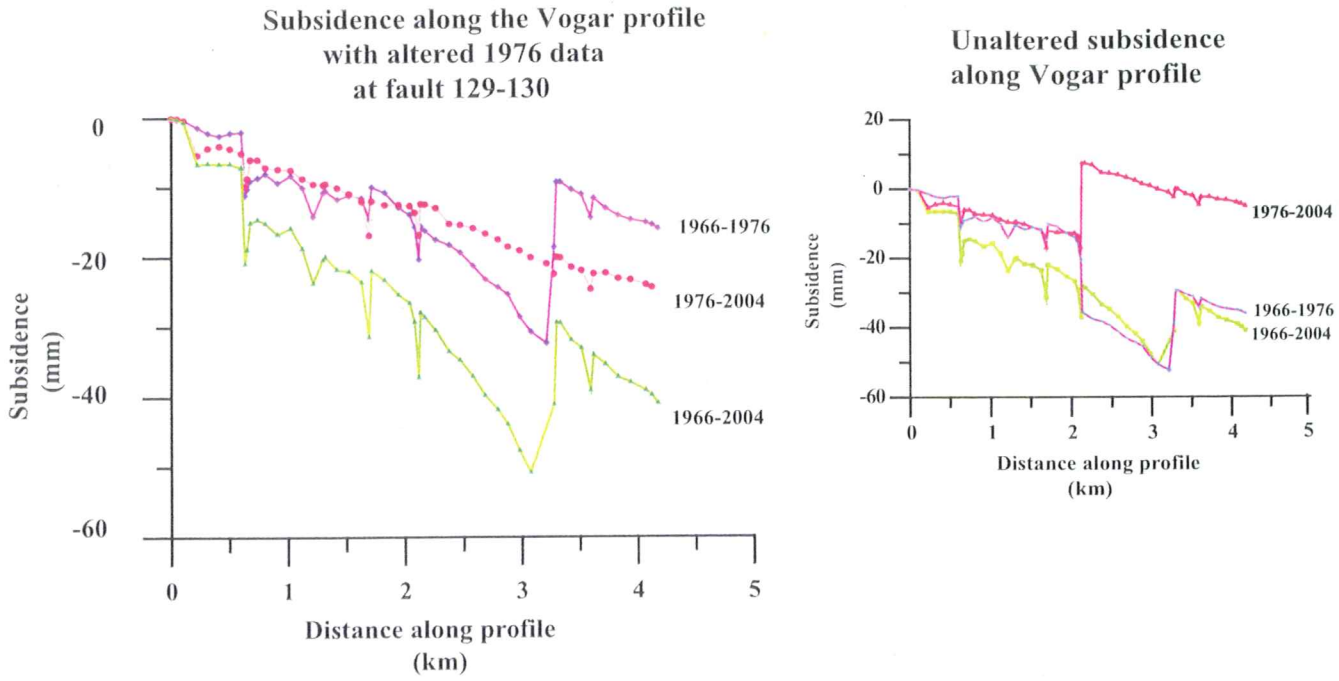

Fig.22. Plot of total subsidence for periods 1966-1976, 1976-2004 and 1966-2004 with altered 1976 data, removing 16mm movement on fault 129-130 between 1966-1976. Second plot shows original values for 1966-1976, 1976-2004 and 1966-2004 for comparison

occurring during the periods, the fault movement on Hrafnagjá between benchmarks 108-111 in the earthquake swarm of 1967 and on faults 129-130 and 141-143, in one of the many earthquake events between 1971 and 1976. The 1976-2004 plot (Fig. 12) shows a subsidence of benchmark 154 relative to benchmark 101 of 0.18mm per year (Table 2). This subsidence is significantly less than that of all other datasets. This low annual average subsidence is the result of a significant, though unconfirmed, fault movement. The 1976-2004 data is displaced up 24mm at fault 129-130, without which the annual subsidence would probably be closer to the average rate over the 38 years of 1.1mm/yr. Substantial fault movements cause annual rates which are perhaps not representative of the average rate of subsidence, as they displace the profile up or down a certain amount.

6.2 Fault Movement

6.2.1 Fault movement in recent data

In the most recent data, fault movements on most faults appear local and have shown similar characteristics during previous time-periods. Local movements are ones affecting only single benchmarks close to faults (see section 6.2.4). A tentative conclusion from this data is that all of these minor movements occurring between 1976 and 2004 are the result of progressive subsidence along lines of weakness. The movement at fault 129-130, however, because of both its relative size and because it has shown no significant movement over the time prior to 1971, could be an earthquake related movement.

6.2.2 The eventual error in the 1976 data

As mentioned, fault movements are confirmed if they are apparent in two separate datasets. For example the fault movement on 141-143 can be seen in both the 1966-2004 and the 1971-1976 datasets, where the data is completely independent from each other. The query, thus, in the specific case of a reverse movement in 1971-1976 followed by an almost equal normal movement in 1976-2004 is that they cancel over the time period 1966-2004. In other words, both movements occurring is indistinguishable from no movement occurring at all. Hence, the movement cannot be confirmed, nor confirmed to be erroneous.

Supporting the suggestion that this single measurement is erroneous is that in the 1976-2004 data, we have an apparent relative "uplift" of the area beyond benchmark 130. During no other time period have we seen this form of uplift at such a distance from benchmark 101. Furthermore, no reverse movements of this magnitude have occurred during any other time period. The setting is tensional and normal faulting is clearly the most frequent form of movement.

One must also consider the fact that stems from the convenience of the data. An erroneous data suggesting reverse movements, affects the succeeding dataset in such as way as to show a normal movement equal to the reverse movement. What are the odds that Nature happens conform to this scenario and produces an almost equal normal movement after a reverse movement between 1971-1976?

If there had not been any reverse movement between 1971 and 1976, then we would not have this relative uplift between 1976 and 2004. In fact the ensuing results of plotting graphs (Fig. 22) disregarding this movement depicts a development more analogous with the rest of the data:

- Between 1971 and 1976 there was a normal movement on the fault 141-143 of ca 20mm
- Between 1976 and 2004 there was a small normal faulting on the 129-130 fault (ca 10mm) and a minor continued faulting on 141-143 (ca 2.5mm).

Other data supporting the suggestion of an erroneous measurement is that average rates of subsidence, when without this fault movement, conform well with the other average rates, bringing 1971-1976 closer to 2.5mm, as in 1966-1968, and 1976-2004 to ca 0.8mm, close to the average over the whole time period. However, like 1966-1968, we know 1971-1976 to be an active period of earthquakes, and accordingly active faulting. Hence, this annual rate of subsidence does not necessarily provide hard evidence supporting an error, or in any way disproving the average rates of subsidence.

The fact that the total subsidence between 1971 and 1976, however, exceeds the total subsidence at some places along the profile between 1966 and 2004, can be seen as valuable evidence (Fig. 22).

One must, however, given the indications supporting an erroneous measurement, also consider the probability of making this erroneous measurement. Once again, the answer dwells in the convenience of the data. What is the probability of an erroneous measurement being made at all, made at a fault, and made both in a way and to a degree as to be theoretically explainable?

Naturally there is no easy answer. Neither case provides hard enough evidence to support either claim. Hence, conclusively, there is no conclusion.

6.2.3 Total fault movement

Three faults on the Vogar profile, 114-115, 115-116 and 123-124, show reverse movements during the 38 year period studied. These three faults are rather small, with total vertical displacements less than 2m. Since fault movements are unlikely to be completely independent, it is probable that these reverse movements on smaller faults are due to the effect of movement at larger faults. Movement of a fault block at one fault causes a tilt, or movement which is reverse at another fault, in essence, either a see-saw effect between two facing faults (Fig. 23) or a block movement between two faults dipping in the same direction (Fig. 13). Also, because there are not many permanent benchmarks across the fault scarps, a completely clear picture is missing.

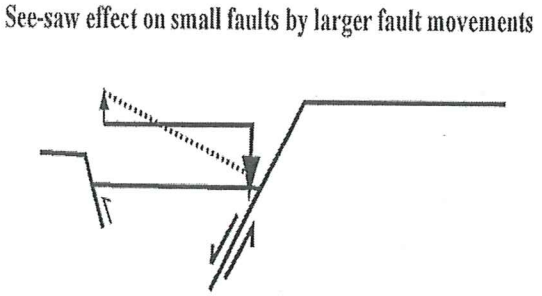

Fig. 23. Diagram showing the effect movement on larger faults may have on smaller faults by a form of see-saw mechanism.

The two main fault movements over the whole time-period are those on faults 108-111 and 141-143, which are faults close to the boundaries of the Vogar graben, which, as mentioned, caused the central part of the fissure swarm to subside.

The movement apparent between benchmarks 103-104 occurs mainly between 1976 and 2004. This could be an up until now undefined fault, assumed to be one of many fractures in the area, or perhaps the effect of inadvertent movement of a fractured block. However, it appears that a block consisting of benchmarks 104-108 has moved as a single unit, subsiding into the Vogar graben feature, probably as a result of earthquake activity.

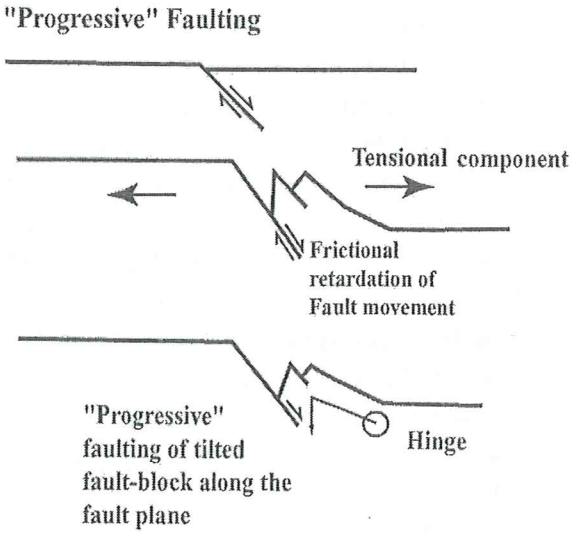

Fig. 24. Simplified diagram of "progressive" faulting occurring at most faults along the profile. Fault movement is frictionally slowed when faulting exceeds spreading, fault block is bent and fractured and then moves at a hinge to slide into place with the rest of the fault block.

6.2.4 Local fault movement

Many of the fault movements appear 'local' on the 1966 to 2004 plot (Fig. 11c), confined to one benchmark on the down-

throw side of the fault. This implies that the there has been no actual movement on the fault so much as the benchmark may have been placed into a part of the fault-block that is fractured and unstable and tilts or moves relative to the ground close to it.

A probable hypothesis is that at some point faulting exceeded spreading in the area, which meant the fault-block on the down-throw side was bent upward on account of frictional forces (Fig. 24) as opposed to moving as a perfect block. In essence, a part of the block is exhibiting a reverse fault movement. As spreading progresses, the faulting occurs by a hinge-fault mechanism, with the upturned fault-block slowly slipping down along the fault plane into level with the down-thrown fault-block. This would give a local subsidence of a single point on the down-throw side. This form of faulting appears to be occurring on faults 108-111, 123-124, 129-130 and 147-148. The fault Hrafnagjá (108-111) clearly exhibits this type of behavior (Fig. 15) at certain locations along the fault. Tryggvason termed the area close to the fault the 'disturbed zone' (Tryggvason 1970). The benchmarks 109-110 are located in this zone. From observations it was reported that this block moved independently during fault movement. Many faults along the profile exhibit similar physical characteristics as Hrafnagjá, with deep fractures having vertical walls and seemingly small vertical displacements giving way to clear fault scarps (Fig. 17, 18). This implies that blocks close to the faults have in many cases been semi-detached along a hinge, tilted and hence act semi-independently along the fault-trace.

The actual fault movement on these faults must then be measured across the subsided benchmark (Table 6).

Table 6. Fault movement across locally affected benchmarks

Fault	1966-2004-Total fault movement (mm)
122-124	1.62
128-130	1.34
146-148	-1.02

Comparing these results one can see that 123-124 (122-124) and 129-130 (128-130) subside visibly less (1.62 and 1.34 compared to 9.48 and 9.25mm) and 147-148 (146-148) actually shows no movement, but simply regional tilting.

6.2.5 Progressive faulting

It is most certainly the case that faulting did not occur exclusively progressively, with small frequent movements. Faulting was in most cases, more substantial at some point. It is apparent that faulting, though not significant on all faults during each time period, is occurring. This faulting is, as we mentioned, in several instances merely local, with a section of the fault block sliding along the fault plane (Fig. 24). Given this one cannot use the data to correlate to the total movement having taken place over 12500 years, since this progressive faulting is in many cases independent of actual fault movement. This type of correlation can only be done on the two boundary faults showing actual fault movement (108-111 and 141-143). On fault 141-143 the rate of movement over the 38 year period could cause the total vertical throw. On fault 108-111 that

rate is barely 1/3rd of that needed for total vertical throw.

Given this data we can infer that although progressive faulting may be occurring at present, each fault must have shown considerable vertical movement at some other time. It is apparent that none of the major faults are completely inactive as subsidence appears to be affecting them each separately. However, the fault movement does not appear to have a constant rate, implying it is subject to periods of varying activity along with considerable faulting at various times.

The only reasonable conclusion to draw from this data is that what we in this paper term 'progressive faulting', is an effect of subsidence from rifting on the Reykjanes peninsula, which causes slight local movement on fault traces given their fractured nature and inherent weakness.

6.3 Earthquake data

Looking over earthquakes since the early 20th century it becomes apparent that the term 'active period' within the region is not completely unsubstantiated given the following;

- **1930-1934 14 events**
- 1935-1937 no events
- **1938-1941 3 events**
- 1942-1944 no events
- **1945-1952 7 events**
- 1953-1955 no events
- **1956-1957 3 events**
- 1958-1963 no events
- **1964-1969 8 events**
- 1970- no events
- **1971-1976 25 events**
- 1976-1989 no events
- **1989-2004 5 events**

The area appears to be characterized by calmer periods in which there is a build up of stress, followed by a period with release of stress.

It is apparent that fault movement and subsidence from 1966-1968 and 1971-1976 have been affected by the greater amount of more substantial earthquakes in the area. It is also apparent that periods with less earthquakes generally have less movement on faults, and hence, often, less subsidence. Earthquakes are the likely reason for the local subsidence of benchmarks by faults where the fault block slips semi-independently along the fault plane at the hinge-line.

The fault block subsidence between faults 129-130 and 141-143 between 1971 and 1976 is probably the result of one or several of the earthquake events during this time period. The subsequent reversal of the 129-130 fault movement between 1976 and 2004 could be the result either of the smaller events within the area between 1976 and 2004 or a result of the large earthquakes in 2000 in the SISZ (Fig. 2). Also noticeable is that the period between 1976 and 2004 is decisively less active considering earthquake activity.

Evidence thus supports fault movements being related to earthquakes. This based on observations indicating more substantial movement during periods of high earthquake activity in the area or some large earthquakes in the extended area.

Progressive fault movement of 'disturbed' blocks occur both during earthquake 'active' periods and less active periods. Given the higher rates of progressive faulting during 'active' earthquake periods it is likely that they are subject to both earthquakes and the

tensional regime, along with, perhaps, the simple effect of gravity.

6.4 Modeling results

Fitting the benchmarks affected by the regional component with the model was possible within the lower parameter values for h_{rift} and d_{lock} values given by I nSAR study (Vadon and Sigmundsson 1997) when disregarding GPS values. Modeling the subsidence in relation to the plate boundary given the GPS data of absolute subsidence of benchmark 106, however, proved too complex for the simple model of linear subsidence. The GPS data for point NAUF fit well with any plot within its error margins. There are three possible scenarios of explain this.

1. GPS data from the VOGA point was obtained during an eleven year period only. The average annual subsidence plot used was for a 38 year period. It is possible that the average vertical subsidence of benchmark 106 during the 38 year period is lower than that suggested by the GPS data for the eleven year period. This in turn could mean that the actual vertical subsidence for benchmark 106 is close to the 0.92mm/yr value, which was obtained from the best model fit of the 1966-2004 data. Rates could on average be higher in the last eleven year period given the earthquakes of 2000.

2. Although points 101-103 and 143-154 appear to be affected almost exclusively by the regional component it is possible that they are also subject to the effect of the local fissure swarm. This could mean that due to the tensional component present in the fissure swarm all points along the profile subside an additional 2mm or more, bringing subsidence of benchmark 106 within the GPS limits. With the data available at present it is not possible to ascertain if this suggestion is conceivable.

3. The final possible explanation is that given the complex geological setting with fissure swarms, areas between fissure swarms, and plate boundary, and this combination of influence from regional and local components that the model is too simple.

6.5 Future scenarios

It is perhaps not easy to speculate about future scenarios, given that although results may match well with models over annual or decennial measurements, it is harder to model our unpredictable future for several thousands of years. However, as always seems the case with nature, there are trends, and though we cannot assume them to be followed, we can suggest ideas presuming that they might.

Since the relative annual rate of subsidence appears relatively constant, there is no cause to claim that it should not continue in such a fashion. This would mean that the area would continue to tilt towards the southeast, at a rate of ca 1mm/yr. Naturally this tilting is bound to change because if it continued indefinitely we would one day find that the Reykjanes rift is surrounded by two vertical walls,

which is of course a ridiculous presumption. Before that it is likely that new lava rises to fill the subsided area.

It is likely that the next few hundred years for the Reykjanes peninsula, could see a turn towards a new volcanic phase. Given that volcanic activity appears to be episodic, occurring ca. every 1000 years (Sigureirsson 1992), and the last phase of activity occurred in the late tenth century to early thirteenth century (Jóhannesson and Einarsson 1998), a new period could be forthcoming. This would mean from anytime soon to some hundred years ahead from now.

However, one must also take into account the in progress ridge jump which is likely to affect the whole geological regime of the Reykjanes peninsula. It is hard to speculate in exactly which ways. Whether, with the slow inactivation of the WVZ the Reykjanes rift and the SISZ join into a single seismic rifting zone, or transcurrent fault, or some hybrid form as visible at the moment on the Reykjanes peninsula, or both are inactivated for some new seismic zone connecting the RR and the EVZ is impossible to tell. When the complete ridge jump is likely to have occurred is also hard to know.

7. Conclusions

Subsidence in the Reykjanes rift zone along the Vogar profile

- Subsidence is occurring toward the central axis of the plate boundary. Subsidence is also occurring within the fissure swarm as a result of two prominent fault movements on boundary faults. The final result is a combination of the effects of both components.

Rates of subsidence along the Vogar profile

- Annual rates of subsidence are not constant and are related to fault movement. Periods of significant fault movements cause rates higher or lower than average depending on the fault orientation.
- The average annual rate of subsidence of the southwest end of the profile over the whole time-period is 1.1 mm/yr.
- The average tilt of the profile over the 38 year period is 0.25μrad.

Fault movement on the Vogar profile

- Larger fault movements are earthquake related. Earthquakes occur mainly in periodic swarms. The period 1976-2004 was a quiet period since substantial stress release occurred between 1971 and 1976 when 25 events occurred within the reference frame defined here.
- Progressive fault movements are occurring on the down-thrown side of several faults. A semi-detached bent block slides along the fault plane bringing about local fault movements.

Model results

- The model for line-source pressure decrease derived from the Mogi model is too simple to account for subsidence in the area, when using GPS data for the VOGA GPS point. The best fit for the points affected by the regional component

is h_{rift} 5.5mm/yr and d_{lock} 3.8km. The subsidence for the VOGA GPS point (benchmark 106) is then 0.92mm/yr.

8. Acknowledgments

I would firstly like to thank my supervisors, Anders Lindh, at Lund University, and Freysteinn Sigmundsson at Nordvulk. Thank you Freysteinn for giving me the wonderful opportunity to come to Iceland, for your help in the field and time at the office. Thank you Anders for the amount of time and commitment, and enthusiasm, you had for my project. Without them this would not have been possible.

Thank you to Haldór Olafsson and Erik Sturkell for letting me help you in the field, the trip to Hekla and above all thank you for the long days of help with my fieldwork.

A big thank you to my new friends, and for a period of time colleagues, at Nordvulk. A special Thanks to Amy Clifton for her help with my map of the profile. Thanks to Þóra Àrnadóttir for sharing the latest GPS results. Thank you Fredrik for dragging me away from my computer for basketball every now and then.

And finally thanks to my friends, my family and to everyone at the geology department for their support, and for putting up with my anti-social behaviour during the last few weeks.

9. References

Clifton, A., Sigmundsson, F., Feig, L., Gudmundsson, G., and Árnadóttir, T., 2002: Surface effects of faulting and deformation at the Hengill triple junction, SW Iceland, 1994-1998. *Journal of Volcanology and Geothermal Research, 115*, 233-255.

Clifton, A., and Schlische, R., 2003: Fracture populations on the Reykjanes peninsula, Iceland: Comparison with experimental clay models of oblique rifting. *Journal of Geophysical Research, 108*, 2074 (ETG **4**-1 - **4**-17).

Clifton, A., Pagli, C., Finndís, J., Jónsdottir, Eythorsdóttir, K., and Vogfjörd, K., 2003: Surface effects of triggered fault slip on Reykjanes peninsula, SW Iceland. *Tectonophysics 369*, 145-154.

Dennis, J.G., 1987: Structural Geology an introduction. Wm. C. Brown Publishers, Dubuque, Iowa.

Einarsson, P., 1991: Earthquake and present-day tectonism in Iceland. *Tectonophysics, 189,* 261-279.

Einarsson, P. and Björnsson, S., 1992: Tectonism, magmatism and earthquakes on the Reykjanes peninsula, Iceland. In *Natural Disasters '92 conference proceeding.* 64-65.

Eysteinsson, H., 1993: Leveling and gravity measurements in the outer part of the Reykjanes peninsula, 1992. *Naural Energy Authority, Report 05 93029.*

Gudsmundsson, G. and Sæmundsson, K., 1980: Statistical analysis of damaging earthquakes and volcanic eruptions in Iceland from 1550-1978.

Journal of Geophysical Research 47, 99-109.

Gudmundsson, S., Sigmundsson, F., and Carstensen, M., 2002: Three-dimensional surface motion maps estimated from combined interferometric synthetic aperature radar and GPS data. *Journal of Geophysical Research, 107*, 2250 (ETG **13**-1 - **13**-14)

Hreinsdóttir, S., 1998: GPS Geodetic Measurements on the Reykjanes Peninsula, SW Iceland: Crustal deformation from 1993 to 1998. *Thesis, Háskóli Íslands,* 1-112.

Hreinsdóttir, S., Einarsson, P., and Sigmundsson, F., 2001: Crustal deformation at the oblique spreading Reykjanes peninsula SW Iceland: GPS measurements from 1993-1998. *Journal of Geophysical Research, 106,* 13803-13816.

Jóhannesson, H., 1980: Jarðlagaskipan of þróun rekbelta á Vesturlandi (evolution of the rift zones in western Iceland). *Náttúrfæðigurinn, 50*, 13-31.

Jóhannesson, H., and Einarsson, S., 1998: Hraun í nágrenni Straumsvíkur (Lava near the Straumsvík area), *Nátturufræðingurinn, 67*, 171-177.

Klein, F., Einarsson, P., and Wyss, M., 1973: Microearthquakes on the Mid-Atlantic plate boundary on the Reykjanes peninsula in Iceland. *Journal Geophysical Research, 78*, 5084-5099-

Klein, F., Einarsson, P., and Wyss, M., 1977: The Reykjanes peninsula, Iceland, earthquake swarm of September 1972 and its tectonic significance. *Journal of Geophysical Research, 82,* 5084-5099.

Mogi, K., 1958: Relations between the eruptions of various volcanoes and the deformation of the ground surface around them. *Bulletin of Earthquake the Research Institute 36*, 99-134.

Pedersen, R., Jónsson, S., Àrnadottir, T., Sigmundsson, F., and Feigl, K., 2003: Fault slip distribution of the two June 2000 M_W 6.5 earthquakes in South Iceland estimated from the joint inversion of the InSAR and GPS measurements. *Earth and Planetary Science Letters 213*, 487-502.

Sturkell, E., Sigmundsson, F., Einarsson, P., and Bilham, R., 1994: Strain accumulation 1986-1992 across the Reykjanes peninsula plate boundary, Iceland, determined from GPS measurements. *Journal of Geophysical Research 21,* 125-128.

Sturkell, E., and Sigmundsson, F., 2000: Continuous deflation of the Askja caldera, Iceland, during the 1983-1998 non-eruptive period. *Journal of Geophysical Research 105,* 25671-25684.

Sæmundsson, K., 1995: Hengill, geological map (bedrock). 1:50000. *Natural Energy Authority*, Reykjavik, Iceland.

Sigmundsson, F., 1996: Crustal deformation at Volcanoes. Environment and climate programme, European school of climatology and natural hazards. The mitigation of Volcanic Hazards, Vulcano Italy 12th-18th June 1994. In Barberi, F., Casale, R, Fartechi, R (editors). *Office of official publications of the European communities.*

Sigmundsson, F., Vadon, H., and Massonnet, D., 1997: Readjustment of the Krafla spreading segment to crustal

rifting measured by satellite radar inferometry. *Geophysical Research Letters, 24,* 1843-1846.

Sigureirsson, M., 1992: Gjósjugos við Reykjnaes á 13. öld (Eruption off the Reykjanes peninsula in the thirteenth century), In *Veggspjaldaráðstefna 48.*

Stefánsson, R., Guðmundsson, G., and Halldórsson, P., 2000: The two large earthquakes in the South Iceland seismic zone on June 17 and 21, 2000. Internet:http://hraun.vedur.is/ja/skyrslur/June17and21_2000/node2.html

Tryggvason, E., 1968: Measurement of Surface Deformation in Iceland by Precision leveling. *Journal of Geophysical Research, 73,* 7039-7050.

Tryggvason, E., 1970: Surface deformation and fault displacement associated with an earthquake swarm in Iceland. *Journal of Geophysical Research. 75.* 4407-4422.

Tryggvason, E., 1974: Vertical crustal movement in Iceland. *Geodynamics of Iceland and North Atlantic area.* Leó Kristjánsson (editor) Dordrecht, Holland, Reidel, 241-262.

Tryggvason, E., 1981: Vertical component of ground deformation in Southwest- and north-Iceland, Result of leveling in 1976 and 1980.

Tryggvason, E., 1982: Recent ground deformation in continental and oceanic rift zones. *Continental and oceanic rifts, Geodetic Series, 8.* 17-29.

Vadon, H., and Sigmundsson, F., 1997: Crustal deformation from 1992 to 1995 at the mid-Atlantic Ridge southwest Iceland, mapped by Satellite Radar Interferometry, *Nature, 275,* 193-197.

SIL Data base:

Internet :http://hraun.vedur.is/cgi-bin/selli (Earthquakes1990-)
http://hraun.vedur.is/ja/ymislegt/storskjalf.html (Earthquakes 1706-1990)

APPENDIX 1. Vogar Profile Coordinates

Numbers in bold are ones which have been altered from the values received to better fit with the profile as drawn by Eysteinn Tryggvason (1968)

Benchmark	**Latitude**			**Longitude**		
	Degrees	Minutes	Seconds	Degrees	Minutes	Seconds
101	-22	-20	-54,1	63	58	35,7
102	-22	-20	-51	63	58	34,9
103	-22	-20	-49,2	63	58	33,3
104	-22	-20	-43,5	63	58	30,5
105	-22	-20	-39,4	63	58	28
106	-22	-20	-36	63	58	25
107	-22	-20	-35,8	63	58	22,2
108	-22	-20	-34,1	63	58	18,9
109	-22	-20	-29,9	63	58	18,6
110	**-22**	**-20**	**-29,7**	**63**	**58**	**18**
111	-22	-20	-29,1	63	58	17,7
112	-22	-20	-26	63	58	16,6
113	-22	-20	-25,9	63	58	13,2
114	-22	-20	-20,9	63	58	10,5
115	-22	-20	-16,7	63	58	7,5
116	-22	-20	-13,9	63	58	4,6
117	-22	-20	-13,8	63	58	1,2
118	-22	-20	-10,2	63	57	59,5
119	-22	-20	**-9,5**	63	57	59
120	-22	-20	-5,9	63	57	55,7
121	-22	-20	**-2,5**	63	57	**52,2**
122	-22	-20	-0,3	63	57	49,1
123	-22	**-19**	**-59**	63	57	47,4
124	-22	-19	-57,8	63	57	**47**
125	-22	-19	-55,5	63	57	45,2
126	-22	-19	-52	63	57	**43**
127	-22	-19	**-51**	63	57	39,9
128	-22	-19	-47,6	63	57	**38,4**
129	-22	-19	**-46**	63	57	**36**
130	-22	-19	**-45**	63	57	**35**
131	-22	-19	**-41**	63	57	**34**
132	-22	-19	-40,3	63	57	30,9
133	-22	-19	-37,8	63	57	27,6
134	-22	-19	-33,4	63	57	25,2
135	-22	-19	-28,6	63	57	21,3
136	-22	-19	-25,9	63	57	18,6
137	-22	-19	-25,7	63	57	15,2
138	-22	-19	***-27,3***	63	57	11,8

Benchmark	Latitude			Longitude		
	Degrees	Minutes	Seconds	Degrees	Minutes	Seconds
139	-22	-19	-22,9	63	57	9,1
140	-22	-19	-21,1	63	57	5,7
141	-22	-19	-17,5	63	57	2,3
142	-22	-19	-12,2	63	57	0,9
143	-22	-19	-10,3	63	57	0,8
144	-22	-19	-9,2	63	56	59,9
145	-22	-19	-9	63	56	56,2
146	-22	-19	-4,2	63	56	54
147	-22	-19	-2,2	63	56	51,9
148	-22	-19	-1,7	63	56	51
149	-22	-18	-55,3	63	56	48,7
150	-22	-18	-51,6	63	56	45,4
151	-22	-18	-47,5	63	56	42,5
152	-22	-18	-43,2	63	56	38,8
153	-22	-18	-39,5	63	56	37,4
154	-22	-18	-40	63	56	35,7

APPENDIX 2. Vogar profile data 2004

Appendix 2, clarifications:

- The Vogar profile was leveled between 7th-10th May 2004.
- A minimum of 4 measurements where obtained, termed 1, 2 ,3 and 4. 1 represents the first measurement taken for each invar rod respectively, 2 the second and so on.
- 1 and 2 were obtained during the forward run, 3 and 4 during the return run
- If the difference between 1 and 2 or 3 and 4 was >0.2mm the measurement was repeated. These new values are also termed measurement 1, 2, 3 or 4. An average value was obtained from the original and the repeated 1 and 2 or 3 and 4 measurement and used for further calculations.
- The average elevation difference between two benchmarks was obtained separately for measurements 1 and 2 and then 3 and 4, by adding the elevation difference for 1 and 2 or 3 and 4 and dividing by two.
- The discrepancy refers to the difference between the average elevation difference obtained from the forward and return run.
- The final value is obtained by dividing the sum of the average elevation difference obtained from the forward and return run by two.

APPENDIX 2. Vogar profile data 2004

Levelled 7/5-10/5 2004
By: Ingrid Anell
Haldór Ólafsson
Freysteinn Sigmundsson
Erik Sturkell

	Forward Measurements					Back Measurements						
	Benchmark		1st meas.	2nd meas.	Diff. 1&2	Average1 (1st+2nd)/2	Benchmark		3rd meas.	4th meas.	Diff 3&4	Average2 (3rd+4th)/2	Disrepency (Av1-Av2)	Total Final Value (Av1+Av2)/2
			(m)	(m)	(m)	(m)			(m)	(m)	(m)	(m)	(m)	(m)
		101	2.64930	2.64927				102	1.45162	1.45155				
		102	1.41149	1.41147				101	2.68918	2.68925				
Diff.101-102			1.23781	1.23780	0.00001	**1.23781**			1.23756	1.23770	-0.00014	**1.23763**	**0.00018**	**1.2377175**
		102	1.50931	1.50916				103	1.33929	1.33931				
		103	1.16098	1.16109				102	1.68729	1.68736				
			0.34833	0.34807	0.00026	0.34820			0.34800	0.34805	-0.00005	0.348025		
		102	1.50922	1.50914										
		103	1.16094	1.16100										
			0.34828	0.34814	0.00014	0.34821								
Diff.102-103						**0.34821**						**0.348025**	**0.00018**	**0.348115**
		103	0.78135	0.78133			103A		0.79972	0.79963				
	103A		0.72821	0.72826				103	0.85263	0.85247				
			0.05314	0.05307	0.00007	0.05311			0.05291	0.05284	0.00007	0.052875		
	103A		1.22743	1.22745			103B		2.36338	2.36318				
	103B		2.31471	2.31460			103A		1.27636	1.2763				
			-1.08728	-1.08715	-0.00013	-1.08722			-1.08702	-1.08688	-0.00014	-1.08695		
	103B		0.73620	0.73630				104	0.80496	0.80504				
		104	0.80192	0.80210			103B		0.73958	0.73959				
			-0.06572	-0.06580	0.00008	-0.06576			-0.06538	-0.06545	0.00007	-0.065415		
Diff.103-104						**-1.09987**						**-1.09949**	**-0.00038**	**-1.09968**
		104	1.55379	1.55379			104A		1.02769	1.02763				
	104A		1.02353	1.02355				104	1.55796	1.55796				
			0.53026	0.53024	0.00002	0.53025			0.53027	0.53033	-0.00006	0.5303		
	104A		2.05748	2.05740			104B		0.35018	0.35021				
	104B		0.36821	0.36827			104A		2.03940	2.03945				
			1.68927	1.68913	0.00014	1.68920			1.68922	1.68924	-0.00002	1.68923		
	104B		2.60230	2.60218				105	0.81969	0.81974				
		105	0.96910	0.96911			104B		2.45278	2.45277				
			1.63320	1.63307	0.00013	1.63314			1.63309	1.63303	0.00006	1.63306		
Diff.104-105						**3.85259**						**3.85259**	**0.00000**	**3.8525875**
		105	0.94186	0.94188			105A		0.86564	0.86564				
	105A		0.89940	0.89946				105	0.90800	0.90787				
			0.04246	0.04242	0.00004	0.04244			0.04236	0.04223	0.00013	0.042295		
	105A		2.49027	2.49026			105B		0.69752	0.69753				
	105B		0.84420	0.84418			105A		2.34371	2.34371				
			1.64607	1.64608	-0.00001	1.64608			1.64619	1.64618	0.00001	1.646185		
	105B		2.27016	2.27012				106	1.32867	1.32867				
		106	1.38782	1.38783			105B		2.21083	2.21087				
			0.88234	0.88229	0.00005	0.88232			0.88216	0.88220	-0.00004	0.88218		
Diff.105-106						**2.57083**						**2.57066**	**0.00017**	**2.570745**
		106	0.85700	0.85699			106A		0.42792	0.42792				
	106A		0.26570	0.26572				106	1.01933	1.01930				
			0.59130	0.59127	0.00003	0.59129			0.59141	0.59138	0.00003	0.591395		
	106A		2.54773	2.54762				107	0.69554	0.69548				
		107	0.71376	0.71378			106A		2.52896	2.52902				
			1.83397	1.83384	0.00013	1.83391			1.83342	1.83354	-0.00012	1.83348		
Diff.106-107						**2.42519**						**2.424875**	**0.00032**	**2.4250325**
		107	2.73669	2.73676			107A		1.74729	1.74721				
	107A		1.63600	1.63599				107	2.84800	2.84808				
			1.10069	1.10077	-0.00008	1.10073			1.10071	1.10087	-0.00016	1.10079		
	107A		1.44814	1.44810				108	0.74432	0.74423				
		108	0.59490	0.59484			107A		1.59737	1.59733				
			0.85324	0.85326	-0.00002	0.85325			0.85305	0.85310	-0.00005	0.853075		
Diff.107-108						**1.95398**						**1.953865**	**0.00012**	**1.9539225**
		108	1.24388	1.24379			108A		2.48769	2.48774				
	108A		2.62220	2.62219				108	1.10911	1.10913				
			-1.37832	-1.37840	0.00008	-1.37836			-1.37858	-1.37861	0.00003	-1.378595		
	108A		0.74683	0.74692			108B		2.88632	2.88643				
	108B		2.72598	2.72608			108A		0.90712	0.90708				
			-1.97915	-1.97916	0.00001	-1.97916			-1.97920	-1.97935	0.00015	-1.979275		
	108B		0.93776	0.93785			108C		2.71677	2.71686				
	108C		2.81175	2.81177			108B		0.84288	0.84282				
			-1.87399	-1.87392	-0.00007	-1.87396			-1.87389	-1.87404	0.00015	-1.873965		
	108C		1.69346	1.69347				109	1.31152	1.31180				
		109	1.27109	1.27106			108C		1.73416	1.73416				
			0.42237	0.42241	-0.00004	0.42239			0.42264	0.42236	0.00028	0.4225		

								109	1.31181	1.31179					
							108C		1.73383	1.73385					
									0.42202	0.42206	-0.00004	0.42204			
												0.42227			
Diff.108-109						-4.80908						-4.809565	0.00049	-4.809323	
		109	0.66304	0.66304			109A		2.70138	2.70139					
	109A		2.77585	2.77586				109	0.58849	0.58849					
			-2.11281	-2.11282	0.00001	-2.11282			-2.11289	-2.11290	0.00001	-2.112895			
	109A		1.65962	1.65962				110	2.79080	2.79080					
		110	2.75132	2.75131			109A		1.69891	1.69892					
			-1.09170	-1.09169	-0.00001	-1.09170			-1.09189	-1.09188	-0.00001	-1.091885			
Diff.109-110						-3.20451						-3.20478	0.00027	-3.204645	
		110	0.30637	0.30638				111	2.70773	2.70769					
		111	2.69336	2.69335				110	0.32083	0.32081					
Diff.110-111			-2.38699	-2.38697	-0.00002	-2.38698			-2.38690	-2.38688	-0.00002	-2.38689	-0.00009	-2.386935	
		111	0.54962	0.54963			111A		1.65579	1.65532					
	111A		1.48092	1.48097				111	0.72408	0.72408					
			-0.93130	-0.93134	0.00004	-0.93132			-0.93171	-0.93124	-0.00047	-0.931475			
	111A		2.16270	2.16264			111A		1.65533	1.65563					
		112	0.59229	0.59229				111	0.72428	0.72427					
			1.57041	1.57035	0.00006	1.57038			-0.93105	-0.93136	0.00031	-0.931205			
								112	0.71068	0.7107		-0.93134			
								111	2.28111	2.2811					
									1.57043	1.57040					
											0.00003	1.570415			
Diff.111-112						0.63906						0.639075	-0.00001	0.6390675	
		112	1.07976	1.07983			112A		0.80469	0.80477					
	112A		0.69357	0.69355				112	1.19067	1.19055	0.00020	0.38588			
			0.38619	0.38628	-0.00009	0.38624			0.38598	0.38578					
	112A		2.41363	2.41349			112A		0.80473	0.80466					
		113	0.56438	0.56444				112	1.19070	1.19062	0.00001	0.385965			
			1.84925	1.84905	0.00020	1.84915			0.38597	0.38596		0.3859225			
	112A		2.41348	2.41344				113	0.53819	0.53793					
		113	0.56432	0.56438			112A		2.38727	2.38719	-0.00018	1.84917			
			1.84916	1.84906	0.00010	1.84911			1.84908	1.84926					
						1.84913									
Diff.112-113						2.23537						2.2350925	0.00027	2.2352288	
		113	2.54930	2.54922			113A		0.62317	0.62325					
	113A		0.63912	0.63916				113	2.53313	2.53307	0.00014	1.90989			
			1.91018	1.91006	0.00012	1.91012			1.90996	1.90982					
	113A		1.75046	1.75057				114	1.38128	1.38119					
		114	1.30822	1.30819			113A		1.82361	1.82356					
			0.44224	0.44238	-0.00014	0.44231			0.44233	0.44237	-0.00004	0.44235			
Diff.113-114						2.35243						2.35224	0.00019	2.352335	
		114	0.64773	0.64774			114A		2.421	2.42082					
	114A		2.31261	2.31273				114	0.75611	0.75608					
			-1.66488	-1.66499	0.00011	-1.66494			-1.66489	-1.66474	-0.00015	-1.664815			
	114A		0.41364	0.41361				115	0.35913	0.35905					
		115	0.37167	0.37142			114A		0.40131	0.40155					
			0.04197	0.04219	-0.00022	0.04208			0.04218	0.04250	-0.00032	0.04234			
	114A		0.41349	0.41368				115	0.35923	0.35909					
		115	0.37159	0.37141			114A		0.40131	0.40134					
			0.04190	0.04227	-0.00037	0.04209			0.04208	0.04225	-0.00017	0.042165			
						0.04208						0.0422525			
Diff.114-115						-1.62285						-1.622563	-0.00029	-1.622708	
		115	2.00231	2.00254			115A		1.62644	1.62636					
	115A		1.61347	1.61327				115	2.01518	2.01526					
			0.38884	0.38927	-0.00043	0.38906			0.38874	0.38890	-0.00016	0.38882			
		115	2.00231	2.00240			115A		1.6264	1.62628					
	115A		1.61349	1.61328				115	2.01521	2.01512					
			0.38882	0.38912	-0.00030	0.38897			0.38881	0.38884	-0.00003	0.388825			
						0.38901		116	2.13122	2.13121		0.3888225			
	115A		1.65777	1.65774			115A		1.65364	1.65364					
		116	2.13537	2.13539					-0.47758	-0.47757	-0.00001	-0.477575			
			-0.47760	-0.47765	0.00005	-0.47763									
Diff.115-116						-0.08861						-0.088752	0.00014	-0.088682	
		116	1.76610	1.76610			116A		0.59226	0.5922					
	116A		0.52773	0.52780				116	1.83046	1.83038					
			1.23837	1.23830	0.00007	1.23834			1.23820	1.23818	0.00002	1.23819			
	116A		1.54047	1.54036				117	1.88234	1.88233					
		117	1.87849	1.87856			116A		1.54405	1.54403					
			-0.33802	-0.33820	0.00018	-0.33811			-0.33829	-0.33830	0.00001	-0.338295			
Diff.116-117						0.90023						0.899895	0.00033	0.90006	
		117	1.61231	1.61227			117A		0.65016	0.65002					
	117A		0.70744	0.70746				117	1.55496	1.55507					
			0.90487	0.90481	0.00006	0.90484			0.90480	0.90505	-0.00025	0.904925			

	117A		2.81380	2.81382			117A		0.64995	0.64989					
		118	1.13628	1.13633				117	1.55498	1.55497					
			1.67752	1.67749	0.00003	1.67751			0.90503	0.90508	-0.00005	0.905055			
						2.58235		118	1.26813	1.26805		0.90499			
							117A		2.94535	2.94537					
									1.67722	1.67732	-0.00010	1.67727			
Diff.117-118						**2.58235**						**2.58226**	**0.00009**	**2.5823025**	
		118	1.56812	1.56805				119	1.06715	1.06723					
		119	1.16816	1.16809				118	1.46702	1.46701					
Diff.118-119			0.39996	0.39996	0.00000	**0.39996**			0.39987	0.39978	0.00009	**0.399825**	**0.00013**	**0.3998925**	
		119	2.08205	2.08210			119A		1.31197	1.31191					
	119A		1.25433	1.25446				119	2.13947	2.13954					
			0.82772	0.82764	0.00008	0.82768			0.82750	0.82763	-0.00013	0.827565			
	119A		2.68264	2.68275			119B		1.61148	1.61134					
	119B		1.44736	1.44736			119A		2.84678	2.84674					
			1.23528	1.23539	-0.00011	1.23534			1.23530	1.23540	-0.00010	1.23535			
	119B		1.39426	1.39439				120	1.66954	1.66956					
		120	1.75018	1.75017			119B		1.31359	1.31362					
			-0.35592	-0.35578	-0.00014	-0.35585			-0.35595	-0.35594	-0.00001	-0.355945			
Diff.119-120						**1.70717**						**1.70697**	**0.00019**	**1.7070675**	
		120	1.99373	1.99397			120A		0.45017	0.4502					
	120A		0.46226	0.46232				120	1.98179	1.98170					
			1.53147	1.53165	-0.00018	1.53156			1.53162	1.53150	0.00012	1.53156			
	120A		1.57095	1.57088				121	1.59090	1.59087					
		121	1.59001	1.58982			120A		1.57194	1.57199					
			-0.01906	-0.01894	-0.00012	-0.01900			-0.01896	-0.01888	-0.00008	-0.01892			
Diff.120-121						**1.51256**						**1.51264**	**-0.00008**	**1.5126**	
		121	2.48639	2.48620			121A		0.49484	0.49497					
	121A		0.53504	0.53502				121	2.44593	2.44596					
			1.95135	1.95118	0.00017	1.95127			1.95109	1.95099	0.00010	1.95104			
	121A		1.74683	1.74690				122	1.35375	1.35380					
		122	1.42965	1.42966			121A		1.6711	1.67114					
			0.31718	0.31724	-0.00006	0.31721			0.31735	0.31734	0.00001	0.317345			
Diff.121-122						**2.26848**						**2.268385**	**0.00009**	**2.26843**	
		122	2.72732	2.72751			122A		0.6343	0.63418					
	122A		0.72594	0.72627				122	2.63539	2.63539					
			2.00138	2.00124	0.00014	2.00131			2.00109	2.00121	-0.00012	2.00115			
	122A		2.60226	2.60216				123	0.68143	0.68150					
		123	0.70586	0.70589			122A		2.57762	2.57762					
			1.89640	1.89627	0.00013	1.89634			1.89619	1.89612	0.00007	1.896155			
Diff.122-123						**3.89765**						**3.897305**	**0.00034**	**3.897475**	
		123	2.88658	2.88667				124	0.78350	0.78346					
		124	0.74517	0.74520				123	2.92472	2.92473					
Diff.123-124			2.14141	2.14147	-0.00006	**2.14144**			2.14122	2.14127	-0.00005	**2.141245**	**0.00020**	**2.1413425**	
		124	1.47456	1.47454			124A		2.59355	2.59372					
	124A		2.64455	2.64474				124	1.42365	1.42389					
			-1.16999	-1.17020	0.00021	-1.17010			-1.16990	-1.16983	-0.00007	-1.169865			
		124	1.47456	1.47443				125	0.71636	0.71605					
	124A		2.64450	2.64447			124A		1.85396	1.85385					
			-1.16994	-1.17004	0.00010	-1.16999			1.13760	1.13780	-0.00020	1.1377			
	124A		1.85063	1.85066		-1.17004		125	0.71623	0.71619					
		125	0.71277	0.71279			124A		1.85381	1.85386					
			1.13786	1.13787	-0.00001	1.13787			1.13758	1.13767	-0.00009	1.137625			
												1.1376625			
Diff.124-125						**-0.03218**						**-0.032202**	**0.00002**	**-0.03219**	
		125	1.65222	1.65219			125A		2.65229	2.65226					
	125A		2.67266	2.67267				125	1.63217	1.63211					
			-1.02044	-1.02048	0.00004	-1.02046			-1.02012	-1.02015	0.00003	-1.020135			
	125A		0.63754	0.63754				126	1.95262	1.95281					
		126	2.02123	2.02121			125A		0.56906	0.56922					
			-1.38369	-1.38367	-0.00002	-1.38368			-1.38356	-1.38359	0.00003	-1.383575			
Diff.125-126						**-2.40414**						**-2.40371**	**-0.00043**	**-2.403925**	
		126	1.73542	1.73535			126A		2.199	2.19881					
	126A		2.22980	2.22975				126	1.70471	1.70468					
			-0.49438	-0.49440	0.00002	-0.49439			-0.49429	-0.49413	-0.00016	-0.49421			
	126A		1.65332	1.65331				127	1.46310	1.46289					
		127	1.45484	1.45492			126A		1.66121	1.66117					
			0.19848	0.19839	0.00009	0.19844			0.19811	0.19828	-0.00017	0.198195			
Diff.126-127						-0.29596						-0.296015	0.00006	-0.295985	
		127	1.44198	1.44187				128	0.58410	0.58409					
		128	0.71150	0.71140				127	1.31464	1.31452					
Diff.127-128			0.73048	0.73047	0.00001	**0.73048**			0.73054	0.73043	0.00011	**0.730485**	**-0.00001**	**0.73048**	
		128	2.28394	2.28425				129	0.58533	0.58544					
		129	0.60981	0.60986				128	2.25948	2.25951					

			1.67413	1.67439	-0.00026	1.67426			1.67415	1.67407	0.00008	1.67411			
		128	2.28418	2.28406											
		129	0.60973	0.60982											
			1.67445	1.67424	0.00021	1.67435									
Diff.128-129						**1.67430**						**1.67411**	**0.00019**	**1.6742063**	
		129	2.85331	2.85334				130	0.97040	0.97041					
		130	1.06721	1.06723				129	2.75676	2.75678					
Diff.129-130			1.78610	1.78611	-0.00001	**1.78611**			1.78636	1.78637	-0.00001	**1.786365**	**-0.00026**	**1.786235**	
		130	2.44100	2.44092				131	1.79365	1.79367					
		131	1.74708	1.74708				130	2.48748	2.48736					
Diff.130-131			0.69392	0.69384	0.00008	**0.69388**			0.69383	0.69369	0.00014	**0.69376**	**0.00012**	**0.69382**	
		131	1.71788	1.71799			131A		1.82418	1.82431					
	131A		1.84844	1.84851				131	1.69352	1.69338					
			-0.13056	-0.13052	-0.00004	-0.13054			-0.13066	-0.13093	0.00027	-0.130795			
	131A		1.31583	1.31584			131A		1.82427	1.82428					
		132	1.01229	1.01235				131	1.69346	1.69343					
			0.30354	0.30349	0.00005	0.30352			-0.13081	-0.13085	0.00004	-0.13083			
								132	0.9066	0.90661		-0.130813			
							131A		1.20974	1.20983					
									0.30314	0.30322	-0.00008	0.30318			
Diff.131-132						**0.17298**						**0.1723675**	**0.00061**	**0.1726713**	
		132	1.13906	1.13902			132A		2.17366	2.17366					
	132A		2.24453	2.24440				132	1.06855	1.06851					
			-1.10547	-1.10538	-0.00009	-1.10543			-1.10511	-1.10515	0.00004	-1.10513			
	132A		2.23004	2.23027				133	1.33292	1.33306					
		133	1.33901	1.33906			132A		2.22373	2.22365					
			0.89103	0.89121	-0.00018	0.89112			0.89081	0.89059	0.00022	0.8907			
Diff.132-133						**-0.21431**						**-0.21443**	**0.00012**	**-0.214368**	
		133	1.44484	1.44484			133A		0.46169	0.46148					
	133A		0.46109	0.46114				133	1.44554	1.44548					
			0.98375	0.98370	0.00005	0.98373			0.98385	0.98400	-0.00015	0.983925			
	133A		1.91207	1.91208				134	1.42309	1.42315					
		134	1.41185	1.41194			133A		1.92311	1.92308					
			0.50022	0.50014	0.00008	0.50018			0.50002	0.49993	0.00009	0.499975			
Diff.133-134						**1.48391**						**1.4839**	**0.00000**	**1.4839025**	
		134	0.78554	0.78566			134A		1.8014	1.80129					
	134A		1.82799	1.82785				134	0.75892	0.75895					
			-1.04245	-1.04219	-0.00026	-1.04232			-1.04248	-1.04234	-0.00014	-1.04241			
		134	0.78581	0.78566				135	2.83167	2.83141					
	134A		1.82835	1.82810			134A		0.64768	0.64701					
			-1.04254	-1.04244	-0.00010	-1.04249			-2.18399	-2.18440	0.00041	-2.184195			
	134A		0.54342	0.54346		-1.04241		135	2.83115	2.83110					
		135	2.72732	2.72736			134A		0.64715	0.64703					
			-2.18390	-2.18390	0.00000	-2.18390			-2.18400	-2.18407	0.00007	-2.184035			
												-2.184115			
Diff.134-135						**-3.22631**						**-3.226525**	**0.00022**	**-3.226415**	
		135	1.39946	1.39952			135A		1.8259	1.82594					
	135A		1.89931	1.89907				135	1.32607	1.32617					
			-0.49985	-0.49955	-0.00030	-0.49970			-0.49983	-0.49977	-0.00006	-0.4998			
		135	1.39938	1.39946				136	0.58053	0.58078					
	135A		1.89953	1.89930			135A		0.92198	0.92168					
			-0.50015	-0.49984	-0.00031	-0.50000			0.34145	0.34090	0.00055	0.341175			
	135A		0.93994	0.93999		-0.49985		136	0.58048	0.58038		0.3414325			
		136	0.59845	0.59847			135A		0.92212	0.92212					
			0.34149	0.34152	-0.00003	0.34151			0.34164	0.34174	-0.00010	0.34169			
Diff.135-136						**-0.15834**						**-0.158368**	**0.00002**	**-0.158355**	
		136	1.37995	1.37978			136A		2.07242	2.07227					
	136A		1.97313	1.97306				136	1.47932	1.47902					
			-0.59318	-0.59328	0.00010	-0.59323			-0.59310	-0.59325	0.00015	-0.593175			
	136A		1.26080	1.26103				137	1.89576	1.89572					
		137	1.76731	1.76733			136A		1.3895	1.38936					
			-0.50651	-0.50630	-0.00021	-0.50641			-0.50626	-0.50636	0.00010	-0.50631			
	136A		1.26098	1.26105				137	1.89584	1.89615		-0.50633			
		137	1.76730	1.76729		-0.50634	136A		1.38961	1.38968					
			-0.50632	-0.50624	-0.00008	-0.50628			-0.50623	-0.50647	0.00024	-0.50635			
Diff.136-137						**-1.09957**						**-1.099505**	**-0.00007**	**-1.099539**	
		137	0.71513	0.71507			137A		1.42455	1.42448					
	137A		1.44722	1.44742				137	0.69241	0.69249					
			-0.73209	-0.73235	0.00026	-0.73222			-0.73214	-0.73199	-0.00015	-0.732065			
		137	0.71194	0.71203				138	0.80205	0.80222					
	137A		1.44410	1.44442			137A		1.1378	1.13777					
			-0.73216	-0.73239	0.00023	-0.73228			0.33575	0.33555	0.00020	0.33565			
	137A		1.13761	1.13777		-0.73225		138	0.80186	0.80211					
		138	0.80213	0.80192			137A		1.13773	1.1375					
			0.33548	0.33585	-0.00037	0.33567			0.33587	0.33539	0.00048	0.33563			
						-0.39658		138	0.80193	0.80169					

							137A		1.13766	1.13767				
									0.33573	0.33598	-0.00025	0.335855		
												0.3357117		
Diff.137-138						**-0.39658**						**-0.396353**	**-0.00023**	**-0.396468**
		138	2.67287	2.67281			138A		0.19798	0.19794				
	138A		0.26001	0.26001				138	2.61109	2.61113				
			2.41286	2.41280	0.00006	2.41283			2.41311	2.41319	-0.00008	2.41315		
	138A		0.96384	0.96390				139	1.27008	1.27025				
		139	1.35065	1.35050			138A		0.88313	0.88325				
			-0.38681	-0.38660	-0.00021	-0.38671			-0.38695	-0.38700	0.00005	-0.386975		
	138A		0.96375	0.96381										
		139	1.35025	1.35047		-0.38664								
			-0.38650	-0.38666	0.00016	-0.38658								
Diff.138-139						**2.02619**						**2.026175**	**0.00001**	**2.0261813**
		139	1.00697	1.00705			139A		0.51819	0.51809				
	139A		0.54300	0.54301				139	0.98256	0.98234				
			0.46397	0.46404	-0.00007	0.46401			0.46437	0.46425	0.00012	0.46431		
	139A		0.78132	0.78161				140	1.10451	1.10471				
		140	1.09450	1.09449			139A		0.79173	0.79171				
			-0.31318	-0.31288	-0.00030	-0.31303			-0.31278	-0.31300	0.00022	-0.31289		
	139A		0.78140	0.78159										
		140	1.09445	1.09455		-0.31302								
			-0.31305	-0.31296	-0.00009	-0.31301								
Diff.139-140						**0.15099**						**0.15142**	**-0.00043**	**0.1512038**
		140	0.82821	0.82829			140A		1.43901	1.43895				
	140A		1.54073	1.54065				140	0.72668	0.72672				
			-0.71252	-0.71236	-0.00016	-0.71244			-0.71233	-0.71223	-0.00010	-0.71228		
	140A		0.97752	0.97757				141	1.42524	1.42485				
		141	1.75413	1.75416			140A		0.64825	0.64816				
			-0.77661	-0.77659	-0.00002	-0.77660			-0.77699	-0.77669	-0.00030	-0.77684		
								141	1.42509	1.42503		-0.776863		
							140A		0.64828	0.64807				
									-0.77681	-0.77696	0.00015	-0.776885		
Diff.140-141						**-1.48904**						**-1.489143**	**0.00010**	**-1.489091**
		141	1.18418	1.18412			141A		1.74768	1.74759				
	141A		2.08306	2.08302				141	0.84906	0.84905				
			-0.89888	-0.89890	0.00002	-0.89889			-0.89862	-0.89854	-0.00008	-0.89858		
	141A		2.74375	2.74366				142	0.19368	0.19365				
		142	0.18966	0.18965			141A		2.7474	2.74751				
			2.55409	2.55401	0.00008	2.55405			2.55372	2.55386	-0.00014	2.55379		
Diff.141-142						**1.65516**						**1.65521**	**-0.00005**	**1.655185**
		142	2.79583	2.79585				143	0.77663	0.77656				
		143	0.79247	0.79245				142	2.77980	2.77986				
			2.00336	2.00340	-0.00004	2.00338			2.00317	2.00330	-0.00013	2.003235		
								143	0.80586	0.80583				
								142	2.80921	2.80921				
									2.00335	2.00338	-0.00003	2.003365		
Diff.142-143						**2.00338**						**2.0033**	**0.00008**	**2.00334**
		143	2.34022	2.34032				144	0.53831	0.53834				
		144	0.62776	0.62773				143	2.25067	2.25065				
Diff.143-144			1.71246	1.71259	-0.00013	**1.71253**			1.71236	1.71231	0.00005	**1.712335**	**0.00019**	**1.71243**
		144	2.14562	2.14558			144A		1.19665	1.19654				
	144A		1.33061	1.33070				144	2.01160	2.01164				
			0.81501	0.81488	0.00013	0.81495			0.81495	0.81510	-0.00015	0.815025		
	144A		1.46469	1.46469			144B		0.99419	0.9941				
	144B		1.24967	1.24972			144A		1.20909	1.2091				
			0.21502	0.21497	0.00005	0.21500			0.21490	0.21500	-0.00010	0.21495		
	144B		2.60184	2.60208			144B		0.99393	0.99418				
		145	0.65866	0.65844			144A		1.20919	1.20917				
			1.94318	1.94364	-0.00046	1.94341			0.21526	0.21499	0.00027	0.215125		
	144B		2.60200	2.60183		1.94351		145	0.80945	0.80941		0.2150375		
		145	0.65833	0.65829			144B		2.7534	2.75332				
			1.94367	1.94354	0.00013	1.94361			1.94395	1.94391	0.00004	1.94393		
Diff.144-145						**2.97345**						**2.9739925**	**-0.00055**	**2.97372**
		145	2.64195	2.64185			145A		1.07484	1.07483				
	145A		1.12993	1.12987				145	2.58681	2.58679				
			1.51202	1.51198	0.00004	1.51200			1.51197	1.51196	0.00001	1.511965		
	145A		1.15708	1.15727				146	1.08566	1.08567				
		146	1.02036	1.02053			145A		1.22261	1.22248				
			0.13672	0.13674	-0.00002	0.13673			0.13695	0.13681	0.00014	0.13688		
						1.64873		146	1.08544	1.0855		0.13695		
							145A		1.22262	1.22236				
									0.13718	0.13686	0.00032	0.13702		
Diff.145-146						**1.64873**						**1.648915**	**-0.00019**	**1.6488225**
		146	1.28799	1.28783			146A		0.31557	0.31537				

	146A		0.28648	0.28636				146	1.31687	1.31699							
			1.00151	1.00147	0.00004	1.00149			1.00130	1.00162	-0.00032	1.00146					
		146	1.28802	1.28784			146A		0.31564	0.31543							
	146A		0.28655	0.28650				146	1.31719	1.31724							
			1.00147	1.00134	0.00013	1.00141			1.00155	1.00181	-0.00026	1.00168					
	146A		2.24364	2.24390		1.00145		147	0.87287	0.87286		1.00157					
		147	0.85635	0.85639			146A		2.26027	2.26019							
			1.38729	1.38751	-0.00022	1.38740			1.38740	1.38733	0.00007	1.387365					
	146A		2.24386	2.24389													
		147	0.85656	0.85662													
			1.38730	1.38727	0.00003	1.38729											
						1.38734											
Diff.146-147						**2.38879**						**2.388935**	**-0.00014**	**2.3888625**			
		147	2.48451	2.48452			147A		0.78334	0.78334							
	147A		0.79393	0.79392				147	2.47331	2.47331							
			1.69058	1.69060	-0.00002	1.69059			1.68997	1.68997	0.00000	1.68997					
	147A		2.00775	2.00773			147B		0.69373	0.69371							
	147B		0.59204	0.59204			147A		2.10946	2.10946							
			1.41571	1.41569	0.00002	1.41570			1.41573	1.41575	-0.00002	1.41574					
	147B		2.88284	2.88273				148	0.75241	0.75237							
		148	0.72284	0.72290			147B		2.91214	2.91213							
			2.16000	2.15983	0.00017	2.15992			2.15973	2.15976	-0.00003	2.159745					
Diff.147-148						**5.26621**						**5.265455**	**0.00075**	**5.26583**			
		148	1.83315	1.83303			148A		2.10398	2.10394							
	148A		2.07049	2.07039				148	1.86642	1.86638							
			-0.23734	-0.23736	0.00002	-0.23735			-0.23756	-0.23756	0.00000	-0.23756					
	148A		0.92049	0.92035			148A		2.10406	2.10402		-0.23757					
		149	0.35347	0.35353				148	1.86637	1.86655							
			0.56702	0.56682	0.00020	0.56692			-0.23769	-0.23747	-0.00022	-0.23758					
	148A		0.92052	0.92064		0.56696		149	0.32943	0.32923							
		149	0.35364	0.35353			148A		0.89636	0.89623							
			0.56688	0.56711	-0.00023	0.56700			0.56693	0.56700	-0.00007	0.566965					
						0.32961		149	0.32927	0.32941		0.5669775					
							148A		0.89644	0.89622							
									0.56717	0.56681	0.00036	0.56699					
Diff.148-149						**0.32961**						**0.3294075**	**0.00020**	**0.3295075**			
		149	1.52853	1.52855			149A		1.31212	1.31203							
	149A		1.34283	1.34277				149	1.49746	1.49753							
			0.18570	0.18578	-0.00008	0.18574			0.18534	0.18550	-0.00016	0.18542					
	149A		1.02661	1.02647				150	1.15697	1.15701							
		150	1.14528	1.14534			149A		1.03808	1.03816							
			-0.11867	-0.11887	0.00020	-0.11877			-0.11889	-0.11885	-0.00004	-0.11887					
	149A		1.02605	1.02622													
		150	1.14519	1.14525													
			-0.11914	-0.11903	-0.00011	-0.11909											
						-0.11893											
Diff.149-150						**0.06681**						**0.06655**	**0.00026**	**0.0666812**			
		150	1.05223	1.05238			150A		0.31083	0.31082							
	150A		0.28411	0.28417				150	1.07897	1.07883							
			0.76812	0.76821	-0.00009	0.76817			0.76814	0.76801	0.00013	0.768075					
	150A		2.63168	2.63185				151	0.89632	0.89629							
		151	0.89896	0.89902			150A		2.6294	2.62931							
			1.73272	1.73283	-0.00011	1.73278			1.73308	1.73302	0.00006	1.73305					
Diff 150-151						**2.50094**						**2.501125**	**-0.00019**	**2.5010325**			
		151	2.43158	2.43163			151A		0.18039	0.1803							
	151A		0.11498	0.11495				151	2.49704	2.49695							
			2.31660	2.31668	-0.00008	2.31664			2.31665	2.31665	0.00000	2.31665					
	151A		2.15178	2.15180			151B		0.26684	0.26679							
	151B		0.54035	0.54031			151A		1.87847	1.87843							
			1.61143	1.61149	-0.00006	1.61146			1.61163	1.61164	-0.00001	1.611635					
	151B		0.95836	0.95790				152	0.07615	0.07610							
		152	0.40442	0.40447			151B		0.62987	0.62984							
			0.55394	0.55343	0.00051	0.55369			0.55372	0.55374	-0.00002	0.55373					
	151B		0.95795	0.95819													
		152	0.40400	0.40430													
			0.55395	0.55389	0.00006	0.55392											
						0.55380											
Diff.151-152						**4.48190**						**4.482015**	**-0.00011**	**4.4819588**			
		152	1.88611	1.88598				153	0.32058	0.32067							
		153	0.37129	0.37133				152	1.83547	1.83551							
Diff.152-153			1.51482	1.51465	0.00017	**1.51474**			1.51489	1.51484	0.00005	**1.514865**	**-0.00013**	**1.5148**			
		153	2.02842	2.02840				154	0.28082	0.28073							
		154	0.23078	0.23086				153	2.07813	2.07812							
Diff.153-154			1.79764	1.79754	0.00010	**1.79759**			1.79731	1.79739	-0.00008	**1.79735**	**0.00024**	**1.79747**			

APPENDIX 3. Vogar Profile Data All Years

	1966			1968			1969		1971			1976		2004	
Benchmark	Elevation difference (cm)	accum. (m)	*minus101*	Elevation difference (cm)	accum. (m)	*minus101*	Elevation difference (cm)	accum. (m)	Elevation difference (cm)	accum. (m)	*minus101*	Elevation difference (cm)	accum. (m)	Elevation difference (cm)	accum. (m)
100	0	0		0	0				0	0					
101	106.8098	1.068098	0	106.1986	1.067986	0	0	0	106.8522	1.068521	0	0	0	0	0
102	123.7899	2.305997	1.237899	123.795	2.305937	1.237951	123.782	1.23782	123.8018	2.30654	1.238019	123.7768	1.237768	123.7718	1.237718
103	34.8529	2.654526	1.586428	34.8317	2.654253	1.586267	34.8335	1.586155	34.8394	2.654934	1.586413	34.8385	1.586153	34.8115	1.585833
104	-109.3571	1.560955	0.492857	-109.4515	1.559737	0.491751	-109.4421	0.491734	-109.4479	1.560454	0.491933	-109.4669	0.491484	-109.968	0.486153
105	385.2429	5.413383	4.345285	385.1917	5.411654	4.343668	385.2129	4.343863	385.1895	5.412349	4.343828	385.1615	4.343099	385.2588	4.338741
106	257.0833	7.984215	6.916117	257.0443	7.982096	6.91411	257.0644	6.914507	257.0732	7.983082	6.914561	257.0419	6.913518	257.0745	6.909486
107	242.5	10.409215	9.341117	242.5133	10.40723	9.339244	242.5222	9.339729	242.5321	10.408402	9.339881	242.541	9.338928	242.5033	9.334519
108	195.445	12.363664	11.295566	195.487	12.3621	11.294114	195.4845	11.294574	195.4794	12.363194	11.294673	195.4569	11.293497	195.3923	11.288442
109	-479.5518	*7.568144*	6.500046	-479.9777	7.562321	6.494335	-480.0882	6.493692	-480.1331	7.561864	6.493343	-480.4569	6.488927	-480.932	6.479122
110	-320.6692	4.361452	3.293354	-320.7072	4.355249	3.287263	-320.6789	3.286903	-320.6677	4.355186	3.286665	-320.5777	3.28315	-320.465	3.274472
111	-239.077	1.97068	0.902582	-239.2115	1.963133	0.895147	-239.1643	0.89526	-239.1256	1.96393	0.895409	-238.9642	0.893508	-238.694	0.887532
112	63.8609	2.60929	1.541192	63.9024	2.602157	1.534171	63.924	1.5345	63.9007	2.602937	1.534416	63.9057	1.532565	63.9068	1.5266
113	223.5763	4.845052	3.776954	223.6271	4.838428	3.770442	223.6486	3.770986	223.6325	4.83926	3.770739	223.635	3.768915	223.5229	3.761829
114	235.3918	7.198969	6.130871	235.4448	7.192875	6.124889	235.4424	6.12541	235.4157	7.193417	6.124896	235.2597	6.121512	235.2335	6.114164
115	-162.3609	5.57536	4.507262	-162.2898	5.569977	4.501991	-162.3067	4.502343	-162.302	5.570395	4.501874	-162.259	4.498922	-162.271	4.491454
116	-8.572	5.489639	4.421541	-8.5683	5.484293	4.416307	-8.5767	4.416576	-8.5936	5.484458	4.415937	-8.7427	4.411495	-8.868	4.402774
117	90.4987	6.394625	5.326527	90.4209	6.388502	5.320516	90.3658	5.320234	90.3596	6.388052	5.319531	90.0867	5.312362	90.006	5.302834
118	257.8963	8.973588	7.90549	257.9495	8.967996	7.90001	257.9681	7.899915	257.99	8.967953	7.899432	258.2386	7.894748	258.2303	7.885137
119	39.9508	9.373096	8.304998	39.9787	9.367782	8.299796	39.973	8.299645	39.9684	9.367636	8.299115	39.9737	8.294485	39.9893	8.28503
120	170.8001	11.08196	10.013862	170.8356	11.076137	10.008151	170.8284	10.007929	170.8137	11.07577	10.007249	170.767	10.002155	170.7068	9.992098
121	151.373	12.594825	11.526727	151.4136	12.590272	11.522286			151.4217	12.589987	11.521466	151.3439	11.515594	151.26	11.504698
122	226.9962	14.864786	13.796688	227.0476	14.860748	13.792762			227.0365	14.860351	13.79183	226.956	13.785154	226.843	13.773128
123	390.5329	18.770114	17.702016	390.5278	18.766025	17.698039			390.491	18.765259	17.696738	390.2318	17.687472	389.7475	17.670603
124	213.1869	20.901981	19.833883	213.2611	20.898635	19.830649			213.342	20.898666	19.830145	213.6427	19.823899	214.1343	19.811946
125	-3.0852	20.871128	19.80303	-3.0448	20.868186	19.8002			-3.0417	20.868256	19.799735	-3.162	19.792279	-3.219	19.779756
126	-240.1856	18.469268	17.40117	-240.1853	18.466331	17.398345			-240.2041	18.466217	17.397696	-240.3975	17.388304	-240.393	17.375826
127	-29.4778	18.174488	17.10639	-29.4603	18.171726	17.10374			-29.4901	18.17131	17.102789	-29.5837	17.092467	-29.599	17.079836
128	73.3185	18.907672	17.839574	73.2941	18.904666	17.83668			73.2903	18.904221	17.8357	73.1445	17.823912	73.048	17.810316
129	168.2118	20.58979	19.521692	168.1817	20.586483	19.518497			168.1408	20.585617	19.517096	167.7433	19.501345	167.4206	19.484522
130	177.6987	22.366775	21.298677	177.7411	22.363891	21.295905			177.7975	22.363602	21.295081	176.1795	21.26314	178.6235	21.270757
131	69.4521	23.061294	21.993196	69.4593	23.058483	21.990497			69.4594	23.058182	21.989661	69.3873	21.957013	69.382	21.964577
132	17.451	23.235801	22.167703	17.4266	23.232746	22.16476			17.407	23.232254	22.163733	17.3172	22.130185	17.2671	22.137248
133	-21.135	23.024448	21.95635	-21.1188	23.021556	21.95357			-21.1552	23.020706	21.952185	-21.2085	21.9181	-21.437	21.922878
134	148.5165	24.509613	23.441515	148.532	24.506874	23.438888			148.5384	24.506088	23.437567	148.4062	23.402162	148.3903	23.406781

	1966			1968			1969		1971			1976		2004	
	Elevation difference (cm)	accum. (m)	*minus101*	Elevation difference (cm)	accum. (m)	*minus101*	Elevation difference (cm)	accum. (m)	Elevation difference (cm)	accum. (m)	*minus101*	Elevation difference (cm)	accum. (m)	Elevation difference (cm)	accum. (m)
135	-322.4076	21.285533	20.217435	-322.3933	21.282939	20.214953			-322.439	21.281693	20.213172	-322.5955	20.176207	-322.642	20.180361
136	-15.5605	21.129924	20.061826	-15.5576	21.127361	20.059375			-15.5893	21.125809	20.057288	-15.7553	20.018654	-15.836	20.022001
137	-109.7556	20.032367	18.964269	-109.7477	20.02988	18.961894			-109.752	20.028275	18.959754	-109.8691	18.919963	-109.954	18.922461
138	-39.4401	19.637966	18.569868	-39.4574	19.635303	18.567317			-39.4753	19.63353	18.565009	-39.5414	18.524549	-39.647	18.525991
139	202.9968	21.66793	20.599832	202.9783	21.665084	20.597098			202.9561	21.663086	20.594565	202.6728	20.551277	202.6181	20.552172
140	15.4342	21.822269	20.754171	15.4246	21.819328	20.751342			15.4128	21.817215	20.748694	15.221	20.703487	0.151204	20.703376
141	-148.6577	20.335689	19.267591	-148.6816	20.332511	19.264525			-148.671	20.330505	19.261984	-148.8209	19.215278	-148.909	19.214286
142	164.2977	21.978664	20.910566	164.2832	21.975341	20.907355			164.2648	21.973145	20.904624	165.6668	20.871946	165.5185	20.869471
143	199.1633	23.970294	22.902196	199.1641	23.96698	22.898994			199.1897	23.965042	22.896521	200.0907	22.872853	200.334	22.872811
144	171.2497	25.682788	24.61469	171.251	25.679489	24.611503			171.2592	25.677643	24.609122	171.2512	24.585365	171.243	24.585241
145	297.6171	28.658958	27.59086	297.5711	28.655197	27.587211			297.585	28.653488	27.584967	297.5082	27.560447	297.372	27.558961
146	164.9966	30.308921	29.240823	164.978	30.304973	29.236987			164.9842	30.303329	29.234808	164.9288	29.209735	164.8823	29.207784
147	239.4917	32.703842	31.635744	239.4755	32.69973	31.631744			239.4573	32.697906	31.629385	239.1585	31.60132	238.8863	31.596647
148	526.0792	37.96463	36.896532	526.0953	37.960678	36.892692			526.0947	37.958847	36.890326	526.3582	36.864902	526.583	36.862477
149	33.0853	38.295478	37.22738	33.0822	38.291496	37.22351			33.068	38.28952	37.220999	32.942	37.194322	32.9508	37.191985
150	6.8619	38.363998	37.2959	6.8127	38.359619	37.291633			6.8203	38.357727	37.289206	6.7465	37.261787	6.6681	37.258666
151	250.1799	40.865791	39.797693	250.203	40.861648	39.793662			250.1732	40.859467	39.790946	250.121	39.762997	250.1033	39.759699
152	448.3078	45.348861	44.280763	448.2921	45.344566	44.27658			448.3032	45.342468	44.273947	448.266	44.245657	448.1959	44.241658
153	151.5518	46.864372	45.796274	151.5314	46.859878	45.791892			151.5397	46.857849	45.789328	151.5195	45.760852	151.48	45.756458
154	179.863	48.663002	47.594904	179.8219	48.658096	47.59011			179.8258	48.655097	47.586576	179.8067	47.558919	179.747	47.553928

APPENDIX 4. Error Calculations Vogar 2004

Benchmarks	Distance between benchmarks* (m)	Accumulated distance (m)	Individual errors (mm)	Total error (mm)
100				
101	0	0		
102	52.3	52.3	0.0457384	0.0457384
103	56	108.3	0.0473286	0.0658179
104	135.3	243.6	0.0735663	0.0987117
105	95.1	338.7	0.0616766	0.1163959
106	127.7	466.4	0.0714703	0.136587
107	98.2	564.6	0.0626738	0.1502797
108	102.4	667	0.064	0.1633401
109	106.1	773.1	0.065146	0.1758522
110	25.2	798.3	0.031749	0.1786953
111	52.3	850.6	0.0457384	0.184456
112	89.5	940.1	0.0598331	0.1939175
113	90.1	1030.2	0.0600333	0.2029975
114	109	1139.2	0.0660303	0.2134666
115	123.4	1262.6	0.0702567	0.224731
116	100.3	1362.9	0.0633404	0.2334866
117	111.6	1474.5	0.0668132	0.242858
118	75	1549.5	0.0547723	0.2489578
119	28.5	1578	0.0337639	0.2512369
120	118.9	1696.9	0.0689638	0.2605302
121	105.3	1802.2	0.0648999	0.2684921
122	115.1	1917.3	0.0678528	0.2769332
123	71.2	1988.5	0.0533667	0.2820284
124	19.2	2007.7	0.0277128	0.2833867
125	120.1	2127.8	0.0693109	0.2917396
126	107.3	2235.1	0.0655134	0.299005
127	106.4	2341.5	0.065238	0.3060392
128	56.2	2397.7	0.0474131	0.3096902
129	46.3	2444	0.0430349	0.312666
130	18.8	2462.8	0.0274226	0.3138662
131	57.2	2520	0.047833	0.3174902
132	106.5	2626.5	0.0652687	0.3241296
133	114.5	2741	0.0676757	0.3311193
134	107.5	2848.5	0.0655744	0.33755
135	125.1	2973.6	0.070739	0.3448826
136	117.7	3091.3	0.0686149	0.3516419
137	113.9	3205.2	0.0674981	0.3580614
138	108.5	3313.7	0.0658787	0.3640714
139	113	3426.7	0.0672309	0.370227
140	116.9	3543.6	0.0683813	0.376489
141	122.5	3666.1	0.07	0.3829412
142	92.3	3758.4	0.0607618	0.3877319
143	31.1	3789.5	0.0352704	0.3893328
144	33.2	3822.7	0.0364417	0.3910345
145	131.8	3954.5	0.0726085	0.3977185
146	107.4	4061.9	0.0655439	0.4030831

147	73.2	4135.1	0.054111	0.4066989
148	61.9	4197	0.0497594	0.4097316
149	118.6	4315.6	0.0688767	0.4154804
150	120.4	4436	0.0693974	0.4212363
151	111.2	4547.2	0.0666933	0.4264833
152	149.4	4696.6	0.0773046	0.4334328
153	68.1	4764.7	0.052192	0.4365639
154	53.3	4818	0.0461736	0.4389989

* The distance between the benchmarks is including the distance via the level.

Tidigare skrifter i serien "Examensarbeten i Geologi vid Lunds Universitet":

124. Sundberg, Sven Birger, 2000: Sedimentationsprocesser och avlagringsmiljö för en kantrygg kring platåleran vid Rydsgårds gods i backlandskapet söder om Romeleåsen, Skåne.
125. Kjöllerström, Anders, 2000: En geokemisk studie av bergartsvariationen på Bullberget i västra Dalarna.
126. Cinthio, Kajsa, 2000: Senglacial och tidigholocen etablering och expansion av lövträd på en lokal i nordvästra Rumänien.
127. Lamme, Sara, 2000: Klimat och miljöförändringar under holocen i Sylarnaområdet, södra svenska Skanderna, baserat på analys av makrofossil och klyvöppningar.
128. Jönsson, Charlotte, 2000: Geologisk och hydro-geologisk modellering av området mellan Bjuv och Söderåsen, nordvästra Skåne.
129. Kleman, Johan, 2001: Utvärdering av den underkambriska litostratigrafin på Österlen, södra Sverige.
130. Sundler, Malin, 2001: En jämförande studie mellan uppmätt och MACRO simulerad pesticidutlakning på ett odlingsfält i Skåne.
131. Grönholm, Anna, 2001: Högtrycksmetabasiter i den södra delen av Mylonitzonen: fältgeologi, petrografi och metamorf utveckling.
132. Ekdahl, Magnus, 2001: En studie av Källsjögranitens deformationsmönster och kinematiska indikatorer inom Ullaredszonen.
133. Axheimer, Niklas, 2001: Middle Cambrian trilobites and biostratigraphy of the Almbacken drill core, Scania, Sweden.
134. Lindén, Mattias, 2001: Proglacial deformation of glaciofluvial sediments during the Pomeranian deglaciation in the Neubrandenburg area, NE Germany.
135. Warnhag, Jon, 2001: A geochemical study of the zoned Pan African Mon Repos intrusion, Central Namibia.
136. Lundmark, Mattias, 2001: Zirkonstudie av Norra Hortens bergarter, SV Sverige.
137. Gunnarson, Rebecka, 2001: Sedimentologisk undersökning av en moränskärning i en djup-vittrad sprickdal på Romeleåsen, Skåne.
138. Karlsson, Christine, 2001: Diagenetic and petro-physical properties of deeply versus moderately buried Cambrian sandstones of the Caledonian foreland, southern Sweden.
139. Eriksson, Mårten, 2001: Bedömning av föroreningsspridning kring en nedlagd bensinstation i Karlaby, sydöstra Skåne.
140. Ljung, Karl, 2001: A paleoecological study of the Pleistocene Holocene transition in the Kap Farvel area, South Greenland.
141. Åkesson, Cecilia, 2001: Undersökning av grundvattenförhållanden i området kring Östra Vemmerlöv, Simrishamns kommun, sydöstra Skåne.
142. Bermin, Jonas, 2001: Modelling Mössbauer spectra of biotite.
143. Mansurbeg, Howri, 2001: Modelling of reservoir quality in quartz-rich sandstones of the Lower Cretaceous Bentheim sandstones, Lower Saxony Basin, NW Germany.
144. Hermansson, Tobias, 2001: Sierggavággeskollans strukturgeologiska utveckling; nyckeln till Sareks berggrundsgeologi.
145. Veres, Daniel-Stefan, 2001: A comparative study between loss on ignition and total carbon analysis on Late Glacial sediments from Atteköps mosse, southwestern Sweden, and their tentative correlation with the GRIP event stratigraphy.
146. Ahlberg, Tomas, 2001: Hydrogeologisk undersökning samt sårbarhetskartering av området kring tre bergborrade grundvattenanläggningar i Simrishamns kommun.
147. Boman, Daniel, 2001: Tektonostratigrafi och deformationsrelaterad metamorfos i norra Kebnekaisefjällen, Skandinaviska Kaledoniderna.
148. Olsson, Stefan, 2002: The geology of the Portobello Peninsula; proposal of a saturated to oversaturated lineage within the Dunedin Volcano, New Zealand.
149. Molnos, Imre, 2002: Petrografi och diagenes i den underkambriska lagerföljden i Skrylle, Skåne.
150. Malmborg, Pär, 2002: Correlation between diagenesis and sedimentary facies of the Bentheim Sandstone, the Schoonebeek field, The Netherlands.
151. Jonsson, Henrik, 2002: Permeability variation in a tidal Jurassic deposit, Höganäs basin, Fennoscandian Border Zone
152. Lundgren, Anders, 2002: Seveskollorna i nord-östra Kebnekaise, Kaledoniderna: metabasiter, graniter och ögongnejser.
153. Sultan, Lina, 2002: Reconstruction of fan-

shaped outwash in front of the Mýrdalsjökull ice cap, Iceland: Architecture and style of sedimentation.

154. Rimša, Andrius, 2002: Petrological study of the metamafic rocks across the Småland-Blekinge Deformation Zone
155. Lund, Magnus, 2002: Anti-slope scarp investigation at Handcar Peak, British Columbia, Canada.
156. Sjöstrand, Lisa: 2003: Early to early Middle Ordovician conodont biostratigraphy of the Tamsalu drill core, central Estonia.
157. Nilsson, Jonas, 2003: Carcharhiniforma hajar från Limhamns kalkbrott.
158. Larsson, Linda M., 2003: Late Triassic and Early Jurassic palynology of the Höganäs Basin and the Ängelholm Trough, NW Scania, Sweden.
159. Sköld, Pia, 2003: Holocen skogshistoria i Stenshuvuds nationalpark, Skånes östra kust, Sverige.
160. Fuchs, M., 2003: Påverkan av sterilisering på gruvsand – en mineralogisk och texturell undersökning.
161. Ljungberg, Julia, 2003. Sierggavággeskollan i gränslandet mellan Sarek och Padjelanta; miljöindikatorer för fjällkedjeberggrundens bildning.
162. Håkansson, Lena, 2003: An architectural element analysis of a large-scale thrust complex, Kanin Peninsula, NW Russia: interaction between the Barents and Kara Sea ice sheets.
163. Davidson, Anja, 2003: Ignimbritenheterna i Barranco de Tiritaña, övre Mogánformationen, Gran Canaria.
164. Näsström, Helena, 2003: Klotdioriten vid Slättemossa, centrala Småland – mineralkemi och genes.
165. Nilsson, Andreas, 2003: Early Ludlow (Silurian) graptolites from Skåne, southern Sweden.
166. Dou, Marion, 2003: Les ferromagnésiens du granite rapakivique de Nordingrå – centre-est de la Suède – composition chimique et stade final de cristallisation.
167. Jönsson, Emma, 2003: En pollenanalytisk studie av råhumusprofiler från Säröhalvön i norra Halland.
168. Alwmark, Carl, 2003: Magmatisk och metamorf petrologi av en mafisk intrusion i Mylonitzonen.
169. Pettersson, Ann, 2003: Jämförande litologisk och geokemisk studie av Sevens amfibolitkomplex i Sylarna och Kebnekaise.
170. Axelsson, Katarina, 2004: Bedömning av potentiell föroreningsspridning från ett avfallsupplag utanför Löddeköpinge, Skåne.
171. Ekestubbe, Jonas, 2004: $^{40}Ar/^{39}Ar$ geokronologi och implikationer för tolkningen av den Kaledoniska utvecklingen i Kebnekaise.
172. Lindgren, Paula, 2004. Tre sensvekofenniska graniter: kontakt- och åldersrelationer samt förekomst av metasedimentära enklaver.
173. Janson, Charlotta, 2004. A petrographical and geochemical study of granitoids from the south-eastern part of the Linderödsåsen Horst, Skåne.
174. Jonsson, Sara, 2004: Structural control of fine-grained granite dykes at the Äspö Hard Rock Laboratory, north of Oskarshamn, Sweden.
175. Ljungberg, Carina, 2004: Belemniters stabila isotopsammansättning: paleomiljöns och diagenesens betydelse.
176. Oster, Jessica, 2004: A stratigraphic study of a coastal section through a Late Weichselian kettle hole basin at Ålabodarna, western Skåne, Sweden.
177. Einarsson, Elisabeth, 2004: Morphological and functional differences between rhamphorhynchoid and pterodactyloid pterosaurs with emphasis on flight.
178. Anell, Ingrid, 2004: Subsidence in rift zones; Analyzing results from repeated precision leveling of the Vogar Profile on the Reykjanes Peninsula, Southwest Iceland

LUNDS UNIVERSITET

Geologiska institutionen
Gentrum för GeoBiosfärsvetenskap
Sölvegatan 12, 223 62 Lund